



Adaptive success history adaptive differential evolution with multi-agent participated competition mechanism

Zhongmin Wang¹ · Qifang Luo² · Chuan Zhang¹ · Shiwei Chen¹ · Jun Yu³ · Mahmoud Abdel-Salam⁴ · Rui Zhong⁵ · Daihong Li¹

Received: 13 April 2025 / Revised: 11 October 2025 / Accepted: 22 October 2025

© The Author(s), under exclusive licence to Springer Science+Business Media, LLC, part of Springer Nature 2025

Abstract

This paper proposes an efficient and improved variant of the success history adaptive differential evolution (SHADE), termed Adaptive SHADE with Multi-agent Participated Competition Mechanism (ASHADE-MPC). The proposed ASHADE-MPC incorporates two key components: (1) a Multi-agent Participated Competition (MPC) mechanism and (2) an adaptive mutation probability. The incorporated MPC mechanism enhances search efficiency and stability by integrating two powerful mutation strategies: DE/cur-to-mean($\mathbf{x}_{idx1}^t, \mathbf{x}_{idx2}^t$)/1 and DE/cur-to-mean($\mathbf{x}_{best}^t, \mathbf{x}_{idx}^t$)/1. Additionally, ASHADE-MPC dynamically adjusts the implementation of DE/best/1 and the multi-agent competition mechanism through a switching probability P to balance local exploitation and global exploration at different optimization stages effectively. Extensive experiments in CEC2017, CEC2020, CEC2022, and seven engineering problems against eleven state-of-the-art optimizers demonstrate the superiority and domination of ASHADE-MPC in different optimization challenges. Furthermore, we apply ASHADE-MPC to the ensemble learning domain to detect the coffee leaf disease, where three high-accuracy deep learning models are fused using an ASHADE-MPC-optimized soft voting scheme. Experimental results confirm that the proposed ASHADE-MPC-Ensemble approach improves the accuracy of 0.952% in accuracy, 0.938% in precision, 0.952% in recall, and 0.952% in F1-score compared to the second-best model, Swin Transformer, which highlights the effectiveness and applicability of ASHADE-MPC in real-world scenarios. The source code of this research can be found at <https://github.com/RuiZhong961230/ASHADE-MPC>.

Keywords Differential Evolution (DE) · Success History Adaptive (SHA) Mechanism · Adaptive mutation probability · Multi-agent Participated Competition (MPC) · Ensemble learning · Coffee leaf disease detection

✉ Rui Zhong
zhongrui@iic.hokudai.ac.jp

Mahmoud Abdel-Salam
mahmoud20@mans.edu.eg

Daihong Li
daihongli@ynau.edu.cn

¹ College of Tropical Crops, Yunnan Agricultural University, Yunnan, China

Zhongmin Wang
zhongminwang@ynau.edu.cn

² College of Artificial Intelligence, Guangxi University for Nationalities, Nanning, China

Qifang Luo
luoqifang@gxun.edu.cn

³ Institute of Science and Technology, Niigata University, Niigata, Japan

Chuan Zhang
2021029@ynau.edu.cn

⁴ Faculty of Computer and Information Science, Mansoura University, Mansoura, Egypt

Shiwei Chen
2023097@ynau.edu.cn

⁵ Information Initiative Center, Hokkaido University, Sapporo, Japan

Jun Yu
yujun@ie.niigata-u.ac.jp

1 Introduction

The rapid advancement of diverse industrial sectors has precipitated increasingly complex challenges, thereby rendering the implementation of optimization algorithms of critical significance [1–3]. Optimization processes are fundamentally characterized by the pursuit of optimal solutions under prescribed constraints, which predominantly encompass practical considerations such as physical principles, geometric limitations, and material characteristics. While conventional methodologies frequently employ gradient-based optimization strategies, their efficacy becomes substantially constrained when addressing intricate problem domains [4, 5]. Therefore, this limitation requires the exploration of new optimization methods to improve the solving ability in complex situations.

In recent years, complex optimization problems have been widely addressed using metaheuristic algorithms (MH) owing to their gradient-independent nature [6–8]. Inspired by principles of nature and biological evolution, these algorithms have gained extensive application, effectively seeking approximate optimal solutions even in the absence of detailed mathematical models [9]. Among various metaheuristic algorithms, the Differential Evolution (DE) algorithm [10] has emerged as a significant tool for solving complex optimization problems because of its simple structure, ease of implementation, and robust global optimization capabilities [11–13]. However, the effectiveness of optimization algorithms is constrained by the "No Free Lunch" theorem (NFL), which posits that no single algorithm can achieve optimal performance across all problem domains [14]. Consequently, to address the diverse challenges posed by a broad spectrum of problems, variants of the original Differential Evolution (DE) algorithm with adaptive parameter settings have been developed by researchers [15, 16]. These enhancements are aimed at enhancing both specific problem-solving efficacies and general optimization performances.

The JADE algorithm, proposed by Zhang and Sanderson in 2009 [17], is regarded as a notable milestone within the domain of adaptive parameter control. The strategy for adaptive parameter control pertaining to the scaling factor F and crossover rate Cr in JADE has been extensively adopted by numerous Differential Evolution (DE) variants and has undergone further development [18–20]. Among these variants, Success History Adaptive DE (SHADE), introduced by Tanabe et al. in 2013 [21], emerges as a prominent example. SHADE has incorporated a memory mechanism for documenting successful historical information, extending upon the foundational adaptive parameter control strategy. This mechanism facilitates SHADE's enhanced efficiency and robustness when addressing intricate optimization

problems. Despite its application across a broad spectrum of optimization challenges, SHADE still encounters limitations in diversifying mutation methods and achieving a more refined equilibrium between exploration and exploitation, resulting in inadequate algorithmic diversity and reduced precision. Consequently, the exploitation of novel mutation operators and improved balancing of algorithmic exploration and exploitation constitutes an area of ongoing and vigorous research [22, 23].

Therefore, this paper presents a novel variant of DE named Adaptive SHADE with Multi-agent Participated Competition Mechanism (ASHADE-MPC). Specifically, the contributions of this research endeavor are two-fold:

1. Introducing the Multi-agent Participated Competition (MPC) Mechanism: Within this framework, two innovative mutation strategies, namely DE/cur-to-mean($\mathbf{x}_{idx1}^t, \mathbf{x}_{idx2}^t$)/1 and DE/cur-to-mean($\mathbf{x}_{best}^t, \mathbf{x}_{idx}^t$)/1, are incorporated, which are inspired by the competitive mechanism in DE [24, 25]. By integrating these strategies, the mechanism successfully maintains population diversity throughout the optimization process. Consequently, it mitigates premature convergence towards the current best individual, thereby minimizing the likelihood of becoming trapped in local optima.

2. Integrating the adaptive mutation probability: Motivated by the efficient exploration-exploitation switch in many optimizers [26, 27], ASHADE-MPC introduces an adaptive mutation probability that facilitates dynamic transitions between DE/best/1 (a potent exploitation mutation strategy) and the aforementioned "Multi-agent Participated Competition Mechanism." This dynamic switching mechanism empowers the algorithm to adeptly modulate the equilibrium between global search and local optimization, based on real-time feedback obtained during the course of the optimization process.

To thoroughly assess the performance of the proposed ASHADE-MPC algorithm, we carried out extensive numerical experiments on multiple benchmark platforms, such as CEC2017, CEC2020, CEC2022, and seven engineering optimization problems. Additionally, we rigorously compared the performance of our proposed algorithm with that of several state-of-the-art optimization algorithms, such as CMA-ES [28], L-SHADE [29], jSO [30], and L-SHADE-cnEpSin [31]. All of these algorithms are widely recognized as highly competitive ones. The experimental results show that the ASHADE-MPC algorithm excels in increasing population diversity and balancing global exploration and local exploitation. This allows it to handle a wider variety of optimization challenges.

Furthermore, ASHADE-MPC is applied to the domain of ensemble learning, leading to the proposal of a novel framework, ASHADE-MPC-Ensemble, for detecting coffee leaf

disease. Specifically, eight pre-trained deep learning models are fine-tuned on a coffee leaf disease dataset sourced from Kaggle, with the aim of effectively capturing domain-specific features. Subsequently, the top three models exhibiting the highest accuracies are selected for inclusion in the ensemble. Within this framework, ASHADE-MPC is utilized to determine the optimal weight distribution among the models, thereby balancing their individual strengths while mitigating weaknesses. Numerical experiments demonstrate the considerable potential of this innovative application of ASHADE-MPC in ensemble learning for addressing real-world challenges.

The rest of this paper is structured as follows: In Sect. 2, we will delve into related works. This section will include introductions to Differential Evolution (DE), JADE, and SHADE. Additionally, a thorough literature review of SHADE will be provided to offer a comprehensive understanding of the existing research in this area. Section 3 will then present a detailed introduction to our proposed ASHADE-MPC algorithm. Section 4 delineates the numerical experiments conducted and the analysis performed using CEC benchmarks. The optimization of engineering problems is discussed in Sect. 5. Section 6 introduces our proposed ASHADE-MPC-Ensemble model specifically tailored for coffee leaf disease detection. Finally, Sect. 7 concludes the paper.

2 Related works

This section presents related works including the introduction of DE, JADE, and SHADE in Sect. 2.1 and a brief literature review of DE in Sect. 2.2. This section covers relevant research efforts, including 2.1, the introduction of the differential evolution (DE) and SHADE algorithms, and 2.2, a literature review of the adaptive parameter control strategies for differential evolution.

2.1 Differential evolution (DE), JADE, and success history adaptive DE (SHADE)

Differential Evolution (DE) [32] was proposed by Storn and Price in 1995. This method, based on populations, uses a stochastic approach to optimization. It has since become a well-known algorithm in the field of evolutionary computation, widely applied to solve complex optimization problems across various disciplines due to its simplicity and effectiveness in exploring solution spaces. The fundamental idea of Differential Evolution is to iteratively update individuals in the population through operations such as initialization, mutation, crossover, and selection, gradually approaching the global optimum solution. The paradigm of DE is demonstrated in Fig. 1.

Initialization: DE performs the initialization process of the population through the application of the formula (1).

$$X = \begin{bmatrix} \mathbf{x}_1 \\ \mathbf{x}_2 \\ \mathbf{x}_3 \\ \vdots \\ \mathbf{x}_N \end{bmatrix} = \begin{bmatrix} x_{11} & x_{12} & \cdots & x_{1D} \\ x_{21} & x_{22} & \cdots & x_{2D} \\ x_{31} & x_{32} & \cdots & x_{3D} \\ \vdots & \vdots & \ddots & \vdots \\ x_{N1} & x_{N2} & \cdots & x_{ND} \end{bmatrix}, \quad (1)$$

$$x_{ij} = \text{rand}() \cdot (\mathbf{ub}_j - \mathbf{lb}_j) + \mathbf{lb}_j$$

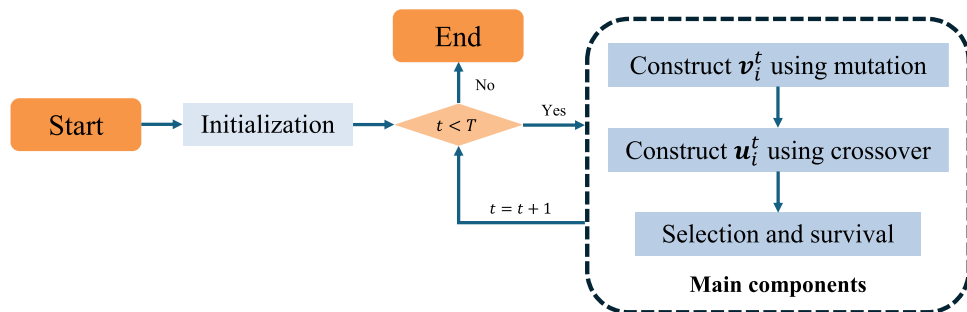
Where X , \mathbf{x}_i , and x_{ij} represent the population, the i^{th} individual, and the j^{th} dimension of \mathbf{x}_i , respectively. The $\text{rand}()$ function yields a random value between 0 and 1.

Mutation: In the population, each member serves as a basis vector. By randomly selecting other members, the algorithm calculates the weighted difference between them to generate a new mutation vector. The weight, which is a user-defined parameter, typically ranges from 0 to 2. Formula (2) illustrates several typical mutation operations.

$$\begin{aligned} \text{DE/rand/1 : } \mathbf{v}_i^t &= \mathbf{x}_{r1}^t + F \times (\mathbf{x}_{r2}^t - \mathbf{x}_{r3}^t) \\ \text{DE/cur/1 : } \mathbf{v}_i^t &= \mathbf{x}_i^t + F \times (\mathbf{x}_{r1}^t - \mathbf{x}_{r2}^t) \\ \text{DE/best/1 : } \mathbf{v}_i^t &= \mathbf{x}_{best}^t + F \times (\mathbf{x}_{r1}^t - \mathbf{x}_{r2}^t) \\ \text{DE/cur-to-best/1 : } \mathbf{v}_i^t &= \mathbf{x}_i^t + F \times (\mathbf{x}_{best}^t - \mathbf{x}_i^t) + F \times (\mathbf{x}_{r1}^t - \mathbf{x}_{r2}^t) \\ \text{DE/cur-to-rand/1 : } \mathbf{v}_i^t &= \mathbf{x}_i^t + F \times (\mathbf{x}_{r1}^t - \mathbf{x}_i^t) + F \times (\mathbf{x}_{r2}^t - \mathbf{x}_{r3}^t) \end{aligned} \quad (2)$$

where \mathbf{x}_i^t and \mathbf{x}_{best}^t represent the i^{th} individual and the best individual in the t^{th} iteration, respectively. \mathbf{x}_{r1}^t , \mathbf{x}_{r2}^t , and \mathbf{x}_{r3}^t

Fig. 1 The paradigm of DE



\mathbf{x}_{r3}^t are three distinct and randomly selected individuals from the population, and F is the mutation factor that controls the scale of the differential vector.

Crossover: In DE, the crossover operation is managed by the crossover rate Cr for the information transfer of mutation vectors between parent and offspring individuals. Taking binomial crossover as an example, its formula is shown as follows (3).

$$\mathbf{u}_{i,j}^t = \begin{cases} \mathbf{v}_{i,j}^t, & \text{if } \text{rand}() < Cr \text{ or } j = j_r \\ \mathbf{x}_{i,j}^t, & \text{else} \end{cases} \quad (3)$$

where j_r is a random integer chosen from $1, 2, \dots, D$, ensure that information from the mutant vector is inherited by at least one dimension of the offspring individual.

Selection: DE employs a basic one-to-one greedy selection strategy to ensure the survival of superior individuals. In the context of the minimization problem, this strategy is reflected in the formula (4).

$$\mathbf{x}_i^{t+1} = \begin{cases} \mathbf{u}_i^t, & \text{if } f(\mathbf{u}_i^t) < f(\mathbf{x}_i^t) \\ \mathbf{x}_i^t, & \text{else} \end{cases} \quad (4)$$

Differential Evolution (DE) is widely utilized across diverse fields owing to its simplicity and efficiency. However, the determination of the F and Cr in DE typically relies on empirical settings, which may not always be conducive to problem-solving when analogous empirical values are applied to disparate issues. Consequently, ascertaining appropriate values for the F and Cr poses a significant challenge. It is apparent that adaptive parameter control holds substantial importance for DE. In 2010, Zhang and Sanderson introduced JADE [17], incorporating adaptive parameters, thereby marking a pivotal advancement in adaptive parameter control for DE algorithms. During each generational update in JADE, the crossover probability Cr_i for an individual x_i is independently generated following a normal distribution with an expectation of μ_{Cr} and a standard deviation of 0.1. Analogously, the mutation factor F_i for an individual x_i is independently produced according to a Cauchy distribution with an expectation of μ_F and a scale parameter of 0.1, where μ_{Cr} and μ_F represent the current set of successful crossover probabilities Cr_i and mutation factors F_i , respectively. These values are computed using Eq. (5).

$$\begin{aligned} F_i &= \text{randn}(\mu_F, 0.1) \\ Cr_i &= \text{randc}(\mu_{Cr}, 0.1) \end{aligned} \quad (5)$$

where $\text{randn}(\mu, \sigma^2)$ and $\text{randc}(\mu, \sigma^2)$ generate random values from normal and Cauchy distributions, respectively, with mean μ and standard deviation σ . Additionally, JADE

incorporates a novel DE/cur-to- p best mutation strategy, as defined in Eq. (6).

$$\mathbf{v}_i^t = \mathbf{x}_i^t + F_i \times (\mathbf{x}_{pbest}^t - \mathbf{x}_i^t) + F_i \times (\mathbf{x}_{r1}^t - \mathbf{x}_{r2}^t) \quad (6)$$

where \mathbf{x}_{pbest}^t refers to an individual randomly chosen from the elite sub-population. After performing mutation and binomial crossover, JADE generates the offspring individual \mathbf{u}_i^t . If \mathbf{u}_i^t has a better fitness than \mathbf{x}_i^t , it replaces the parent, and the corresponding F_i and Cr_i values are stored in the success history S_F and S_{Cr} , respectively. Otherwise, the offspring \mathbf{u}_i^t is discarded. At the end of the iteration, JADE updates the historical memory of μ_F and μ_{Cr} using Eq. (7).

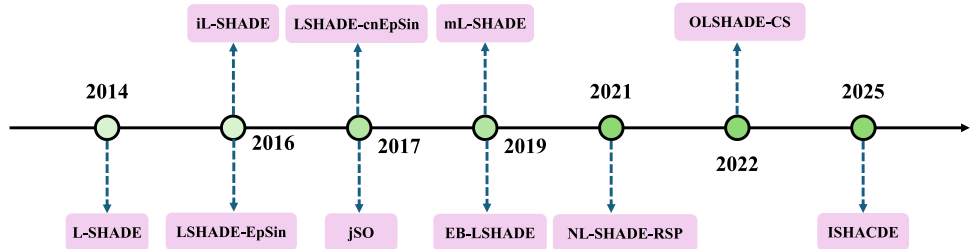
$$\begin{aligned} \mu_F &= (1 - c) \cdot \mu_F + c \cdot \text{mean}_L(S_F) \\ \mu_{Cr} &= (1 - c) \cdot \mu_{Cr} + c \cdot \text{mean}(S_{Cr}) \\ \text{mean}_L(S_F) &= \frac{\sum_{k=1}^{|S_F|} S_{F,k}^2}{\sum_{k=1}^{|S_F|} S_{F,k}} \end{aligned} \quad (7)$$

where $\text{mean}_L(S_F)$ and $\text{mean}(S_{Cr})$ represent the Lehmer mean of S_F and the geometric mean of S_{Cr} , respectively. The parameter $c \in [0.05, 0.2]$ is used to control the balance between the historical memory and the success experience. In the JADE algorithm, the adjustment of the F and CR is based on the statistical information of the success parameters. Specifically, these parameters are dynamically adjusted by calculating the mean values μ_F and μ_{CR} of the success parameters. Although this singular memory mechanism is both simple and effective, in the context of complex optimization problems, the problem characteristics may undergo alterations throughout the progression of the optimization process. However, the adjustment mechanism predicated on the mean value manifests a pronounced lag phenomenon and lacks the capacity to adapt expeditiously to these alterations. To augment the robustness of the JADE algorithm in addressing a diverse array of optimization challenges, Tanabe and Fukunaga [21] introduced an innovative differential evolution algorithm termed Success-History based Adaptive Differential Evolution (SHADE). The key innovation of this algorithm resides in the incorporation of a success-history adaptive mechanism. This mechanism possesses the capability to document the parameter configurations that have proven successful during the optimization process—including the scaling factor F and the crossover rate CR —and utilizes this historical data to inform subsequent parameter adjustments, ultimately enhancing the overall performance of the algorithm. As illustrated in Fig. 2, the success-history adaptive mechanism fulfills its function by establishing a historical memory within the framework of the optimization process.

Fig. 2 Historical memory of μ_F and μ_{Cr}

Index	1	2	3	4	...	H
μ_F	$\mu_{F,1}$	$\mu_{F,2}$	$\mu_{F,3}$	$\mu_{F,4}$...	$\mu_{F,H}$
μ_{Cr}	$\mu_{Cr,1}$	$\mu_{Cr,2}$	$\mu_{Cr,3}$	$\mu_{Cr,4}$...	$\mu_{Cr,H}$

Fig. 3 Representative variants of SHADE in the literature review



where H is the memory length, $\mu_{F,i}$ and $\mu_{Cr,i}$ ($i \in [1, H]$) are set to 0.5 initially. In each iteration, SHADE randomly selects two indices $r1, r2$ from the historical memory and generates new control parameters based on the corresponding $\mu_{F,r1}$ and $\mu_{Cr,r2}$ values. the mutation factor F_i and crossover rate Cr_i are generated using Eq. (8).

$$\begin{aligned} F_i &= \text{randn}(\mu_{F,r1}, 0.1) \\ Cr_i &= \text{randc}(\mu_{Cr,r2}, 0.1) \end{aligned} \quad (8)$$

Similarly, if the newly generated offspring \mathbf{u}_i^t outperforms its parent \mathbf{x}_i^t , the corresponding F_i and Cr_i values are stored in the sets S_F and S_{Cr} . At the end of each iteration, SHADE updates the historical memory parameters $\mu_{F,r1}$ and $\mu_{Cr,r2}$ using Eq. (9).

$$\begin{aligned} \mu_{F,r1} &= (1 - c) \cdot \mu_{F,r1} + c \cdot \text{mean}_{WL}(S_F) \\ \mu_{Cr,r2} &= (1 - c) \cdot \mu_{Cr,r2} + c \cdot \text{mean}_{WA}(S_{Cr}) \\ \text{mean}_{WL}(S_F) &= \frac{\sum_{k=1}^{|S_F|} w_k \cdot S_{F,k}^2}{\sum_{k=1}^{|S_F|} w_k \cdot S_{F,k}} \\ \text{mean}_{WA}(S_{Cr}) &= \sum_{k=1}^{|S_{Cr}|} w_k \cdot S_{Cr,k}^2 \\ w_k &= \frac{\Delta f_k}{\sum_{k=1}^{|S_F|} \Delta f_k} \\ f_k &= |f(\mathbf{u}_i^t) - f(\mathbf{x}_i^t)| \end{aligned} \quad (9)$$

where $\text{mean}_{WL}(S_F)$ and $\text{mean}_{WA}(S_{Cr})$ denote the weighted Lehmer mean of S_F and the weighted geometric mean of S_{Cr} . Weights are calculated based on the improvements between \mathbf{u}_i^t and \mathbf{x}_i^t . By introducing a success-history adaptive mechanism, the SHADE algorithm is able to

record and utilize past successful parameter configurations to dynamically adjust control parameters F and CR . This method not only reduces dependency on initial parameter settings but also enhances the algorithm's adaptability and flexibility. Through the update mechanism of weighted averages, SHADE can better adapt to the dynamic changes of optimization problems, thus achieving a better balance between global search and local optimization.

2.2 Literature review of SHADE

This section presents a brief literature review of representative variants of SHADE, which are listed in Fig. 3.

In 2014, Tanabe and Fukunaga [29] proposed **L-SHADE**, an enhanced version of the SHADE algorithm. It boosts SHADE's performance by integrating a Linear Population Size Reduction (LPSR) mechanism. This mechanism linearly shrinks the population size. In the early optimization stages, it enables the algorithm to explore the solution space widely. Later on, it helps focus on refining the high-quality solutions. As a result, it speeds up convergence and balances exploration and exploitation during the entire optimization process.

In 2016, Brest et al. [33] proposed **iL-SHADE**, an improved version of L-SHADE. iL-SHADE leverages historical memory values from the previous generation to compute those for the next. This allows the algorithm to better inherit and utilize past successful parameter setups, improving parameter tuning accuracy and adaptability. Also, in iL-SHADE, the p-value in the DE/current-to-pbest/1 strategy linearly decreases. This preserves high population diversity early in optimization and focuses on refining high-quality solutions later, speeding up convergence. Building on L-SHADE, Awad et al. [34] introduced the LSHADE-EpSin

algorithm with a new sinusoidal parameter adjustment method. It combines non-adaptive sinusoidal decay and history-based sinusoidal increment. This approach keeps high population diversity initially and then hones in on the discovered high-quality solutions, thus accelerating convergence.

In 2017, Brest et al. [30] proposed **jSO** based on iLSHADE. They applied a lower scale factor in the early iterative optimization stages and a higher one in the later stages. This approach balanced the algorithm's exploration and exploitation. Meanwhile, Awad et al. [31] developed LSHADE-cnEpSin from LSHADE-EpSin. The **LSHADE-cnEpSin** algorithm incorporates sinusoidal perturbations, helping it avoid local optima and explore a wider solution space. Moreover, it uses the concept of Euclidean neighborhood, introducing a neighborhood idea for population individuals. By interacting with nearby individuals, the search quality is improved.

In 2019, Mohamed et al. [35] proposed **EB-LSHADE**. This algorithm introduced two mutation strategies: DE/current-to-ord-best/1 (ord-best) and DE/current-to-ord-pbest/1 (ord-pbest). The former randomly selects three vectors to boost the algorithm's exploration, while the latter chooses the global best vector to improve its exploitation.

In 2021, Stanovov et al. [36] introduced the **NL-SHADE-RSP** algorithm. This algorithm utilizes non-linear population size reduction, rank-based selective pressure, adaptive use of the archive set, and dynamic control of the crossover rate. These features significantly boost the performance of Differential Evolution (DE) in single-objective optimization tasks. Thanks to its capacity for balancing exploration and exploitation, **NL-SHADE-RSP** is highly efficient in tackling complex multimodal problems.

In 2022, Kumar et al. [37] proposed a novel DE variant, **OLSHADE-CS**. It constructs the initial population via orthogonal array and neighborhood search-based initialization methods. Besides, **OLSHADE-CS** utilizes a conservative selection scheme and integrates multiple mutation strategies. The orthogonal array initialization along with neighborhood search helps generate a high-quality initial population. Meanwhile, the integration of multiple mutation strategies and parameter adaptive techniques enables dynamic adjustment of the algorithm's behavior during the search process. The conservative selection scheme plays a crucial role in ensuring the continuous optimization of the population.

In 2025, the **ISHACDE** [38] algorithm introduced an independent successful history adaptation mechanism on the basis of CDE, inheriting the assumptions about the scaling factor (F) and crossover rate (CR) from SHADE, and further hypothesizing that independent evolution of F in

CDE might perform better, thus adjusting F independently. It adopts the DE/winner-to-best/1 mutation operator, combining the advantages of the DE/rand-to-best/1 and DE/current-to-best/1 mutation strategies, intelligently selects mutation strategies based on individual competition relationships, and achieves a dynamic balance between global exploration and local exploitation.

3 Our proposal: ASHADE-MPC

This section provides an in-depth introduction to the proposed ASHADE-MPC, where the flowchart is presented in Fig. 4.

ASHADE-MPC is constructed upon the foundational infrastructure of SHADE, preserving its core components such as population and parameter initialization, mutation operators, crossover operators, selection processes, SHADE-based parameter adaptation, and iterative optimization techniques. The primary distinction between ASHADE-MPC and SHADE lies in the incorporation of a multi-agent participated competition mechanism(MPC) and an adaptive mutation probability. By integrating this multi-agent participated competition mechanism with an adaptive mutation probability, ASHADE-MPC achieves an autonomous equilibrium between exploration and exploitation. This capability enables ASHADE-MPC to dynamically alternate between global search strategies and local optimization tactics, thereby allowing the algorithm's search behavior to adaptively align with the specific requirements of various stages within the optimization process.

During the design phase of ASHADE-MPC, our proposed Multi-agent Participated Competition Mechanism introduced two novel mutation operations: DE/cur-to-mean($\mathbf{x}_{idx1}^t, \mathbf{x}_{idx2}^t$)/1 and DE/cur-to-mean($\mathbf{x}_{best}^t, \mathbf{x}_{idx}^t$)/1. These were seamlessly integrated with the existing DE/cur-to-best/1 mutation operator. Notably, DE/cur-to-mean($\mathbf{x}_{idx1}^t, \mathbf{x}_{idx2}^t$)/1 and DE/cur-to-mean($\mathbf{x}_{best}^t, \mathbf{x}_{idx}^t$)/1 mitigate the reliance on the best individual, thereby preventing premature convergence of the population towards a local optimal solution. Consequently, the population can explore diverse high-quality solution spaces rather than focusing excessively on a single area. As the optimization progresses, the algorithm progressively increases the proportion of DE/best/1 mutation operators through adaptive mutation probability adjustments, facilitating refined development of the current solution and further enhancing its quality.

The update formula of the Multi-agent Participated Competition Mechanism is shown in Eq.(10).

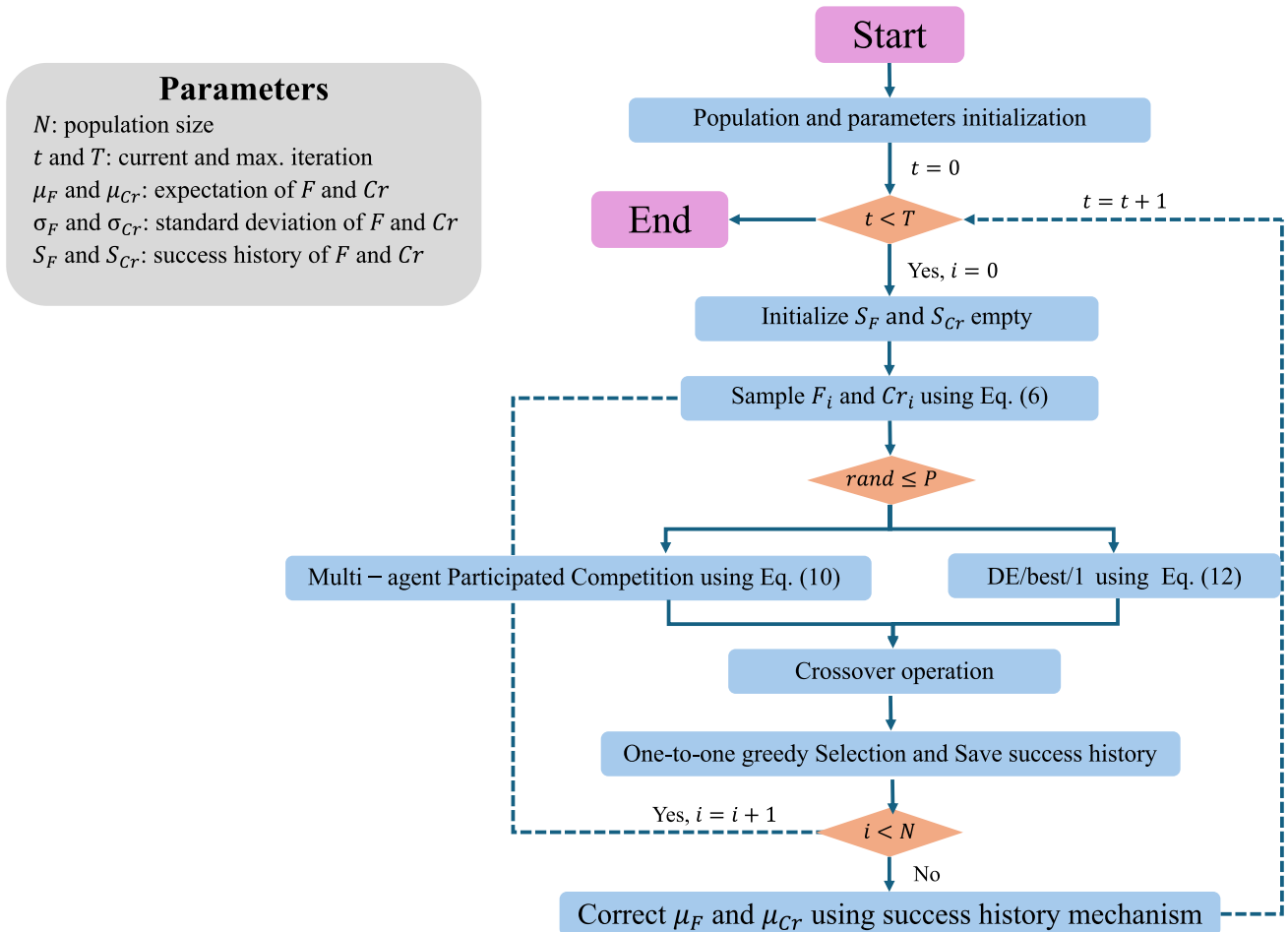


Fig. 4 The flowchart of ASHADE-MPC

$$\mathbf{v}_i^t = \begin{cases} \mathbf{x}_i^t + F (\text{mean}(\mathbf{x}_{idx1}^t, \mathbf{x}_{idx2}^t) - \mathbf{x}_i^t) + F_1 \times (\mathbf{x}_{r1}^t - \mathbf{x}_{r2}^t), \\ \text{if } f(\mathbf{x}_i^t) > \max(f(\mathbf{x}_{idx1}^t), f(\mathbf{x}_{idx2}^t)), \# \text{DE/cur-to-mean}(\mathbf{x}_{idx1}^t, \mathbf{x}_{idx2}^t)/1 \\ \mathbf{x}_i^t + F \times (\mathbf{x}_{best}^t - \mathbf{x}_i^t) + F_1 \times (\mathbf{x}_{r1}^t - \mathbf{x}_{r2}^t), \text{if } f(\mathbf{x}_i^t) < \min(f(\mathbf{x}_{idx1}^t), f(\mathbf{x}_{idx2}^t)), \# \text{DE/cur-to-best}/1 \\ \mathbf{x}_i^t + F (\text{mean}(\mathbf{x}_{best}^t, \mathbf{x}_{idx}^t) - \mathbf{x}_i^t) + F_1 \times (\mathbf{x}_{r1}^t - \mathbf{x}_{r2}^t), \text{otherwise}, \# \text{DE/cur-to-mean}(\mathbf{x}_{best}^t, \mathbf{x}_{idx}^t)/1 \end{cases} \quad (10)$$

where \mathbf{x}_i^t is the position vector of the i -th individual at iteration t , \mathbf{v}_i^t is the mutation vector generated for the i -th individual, F is the scaling factor controlling the intensity of differential vectors, \mathbf{x}_{idx1}^t and \mathbf{x}_{idx2}^t are the competitive position vectors of two different individuals randomly selected from the population, idx is randomly determined between $idx1$ and $idx2$, \mathbf{x}_{r1}^t and \mathbf{x}_{r2}^t are randomly selected individuals for introducing stochastic perturbations, \mathbf{x}_{best}^t is the position vector of the best-fit individual in the current population, $f(\mathbf{x})$ is the fitness function evaluating solution quality for a minimization problem, and $\text{mean}(\cdot)$ denotes the arithmetic mean operation on input vectors.

Secondly, this study uses the formula Eq.(11) to define the adaptive mutation probability p :

$$P = 1 - t/T \quad (11)$$

where t is the current iteration, T is the maximum iteration. If the random number $rand$ is less than P , the individual will be updated according to formula Eq.(10); otherwise, it will be updated using formula DE/best/1. The updating process follows formula Eq.(12).

$$\mathbf{x}_{best}^t + F \times (\mathbf{x}_{r1}^t - \mathbf{x}_{r2}^t) \quad (12)$$

In summary, the pseudocode of ASHADE-MPC is presented in Algorithm 1.

Input: Population size: N , Dimension: D , Maximum evaluations: FE_{\max}
Output: Optimum: $\mathbf{x}_{\text{best}}^t$

```

1 Function ASHADE-MPC( $N, D, FE_{\max}$ ):
2   Initialize parameters and population
3    $t = 0, FE = 0$ 
4   Record  $\mathbf{x}_{\text{best}}^t$ 
5   while  $FE < FE_{\max}$  do
6     Initialize success history memory
7     Sample  $\mu_{F,r}$  and  $\mu_{F,r}$  from historical memory
8     Generate adaptive probability  $P$  via formula (10)
9     for  $i = 0$  to  $N$  do
10       Randomly sample distinct indices  $idx1, idx2, r1, r2 \in \{0, 1, \dots, N - 1\} \setminus \{i\}$ 
11       if  $rand < P$  then
12         if  $f(\mathbf{x}_i^t) > \max(f(\mathbf{x}_{idx1}^t), f(\mathbf{x}_{idx2}^t))$  then
13            $\mathbf{v}_i^t = \mathbf{x}_i^t + F \left( \text{mean}_{\mathbf{x}_{idx1}^t, \mathbf{x}_{idx2}^t} - \mathbf{x}_i^t \right) + F_1 \times (\mathbf{x}_{r1}^t - \mathbf{x}_{r2}^t)$ 
14         end
15         else if  $f(\mathbf{x}_i^t) < \min(f(\mathbf{x}_{idx1}^t), f(\mathbf{x}_{idx2}^t))$  then
16            $\mathbf{v}_i^t = \mathbf{x}_i^t + F_1 \times (\mathbf{x}_{\text{best}}^t - \mathbf{x}_i^t) + F_1 \times (\mathbf{x}_{r1}^t - \mathbf{x}_{r2}^t)$ 
17         end
18         else
19           Randomly select an index from  $idx1$  and  $idx2$  and assign it to  $idx$ 
20            $\mathbf{v}_i^t = \mathbf{x}_i^t + F \left( \text{mean}(\mathbf{x}_{\text{best}}, \mathbf{x}_{idx}^t) - \mathbf{x}_i^t \right) + F_1 \times (\mathbf{x}_{r1}^t - \mathbf{x}_{r2}^t)$ 
21         end
22       end
23       else
24          $\mathbf{v}_i^t = \mathbf{x}_{\text{best}}^t + F \times (\mathbf{x}_{r1}^t - \mathbf{x}_{r2}^t)$ 
25       end
26       Update historical memory using the SHA mechanism
27     end
28     Record  $\mathbf{x}_{\text{best}}^t$ 
29      $t \leftarrow t + 1$ 
30   end
31   return  $\mathbf{x}_{\text{best}}^t$ 

```

Algorithm 1 ASHADE-MPC

Based on the ASHADE-MPC algorithm's pseudocode, we conduct a systematic analysis of its computational complexity. To ensure clarity, we first highlight the essential parameters: the population size is denoted by N , the dimensionality of the search space is D , and the maximum number of iterations allowed is T . The computational complexity of the primary components within ASHADE-MPC is analyzed as follows:

- Parameters and the population initialization: $O(N \times D)$.
- Success history memory initialization: $O(T)$.
- Historical memory sampling: $O(T)$.
- Construct \mathbf{v}_i^t with mutation operator: $O(T \times N \times D)$.
- Selection and success history storage: $O(T \times N)$.
- Historical memory update: $O(T)$.

The complete computational complexity of ASHADE-MPC is computed using Eq. (13).

$$O(N \times D + T \times (3 + N \times D + N)) := O(T \times N \times D) \quad (13)$$

Within the SHADE framework, an elite archive is maintained to facilitate the DE/current-to-pbest/1 mutation strategy. This mechanism requires selecting the top p individuals based on their fitness values, which introduces an additional sorting step and increases computational overhead. Consequently, the computational complexity of SHADE is bounded by $O(T \times N \times \log N \times D)$. In comparison, the proposed ASHADE-MPC method achieves lower computational cost while maintaining competitive performance. This reduction in complexity highlights the enhanced

computational efficiency of ASHADE-MPC over the original SHADE.

4 Numerical experiments in CEC benchmarks

This section presents a comprehensive overview of the numerical experiments performed on CEC benchmarks to assess the overall performance of the proposed ASHADE-MPC algorithm. In Sect. 4.1, we detail the experimental configurations, encompassing both the computational environment and implementation specifics, to ensure the reproducibility and transparency of our research. Section 4.2 outlines the baseline optimizers and their respective

Table 1 Parameter of competitor algorithms

MAs	Parameters	Value
DE	Mutation scheme	DE/cur-to-rand/1
	Scaling factor F	0.9
	Crossover rate Cr	0.9
PSO	Inertia factor w	0.4
	Acceleration coefficients c_1 and c_2	2.05
	Max. and min. speed	2, -2
CMA-ES	Population size N	50
	σ	1.3
	N_{max} and N_{min}	18 D and 4
L-SHADE	μ_F and μ_{Cr}	0.5 and 0.5
	σ_F and σ_{Cr}	0.1 and 0.1
	Population size N	200
jSO	ϕ	0.15
	N_{max} and N_{min}	12 × D and 4
	p_{max} and p_{min}	0.25 and 0.125
L-SHADE-cnEpSin	M_F	0.3
	N_{max} and N_{min}	18 × D and 4
	μ_F and μ_{Cr}	0.5 and 0.5
MCSO	σ_F and σ_{Cr}	0.1 and 0.1
	Memory size H	5
	ps and pc	0.5 and 0.4
L-SHACSO	Population size N	150
	φ_1 and φ_2	0.2 and 0.2
	N_{max} and N_{min}	400 and 4
CDE	μ_ϕ	0.3
	Memory size H	5
	N	100
ISHACDE	μ_F and μ_{Cr}	0.5 and 0.5
	σ_F and σ_{Cr}	0.1 and 0.1
	Memory size H	10
ASHADE-MPC	N	100
	μ_F and μ_{Cr}	0.5 and 0.5
	Memory size H	10
ASHADE-MPC	Population size N	50
	μ_F and μ_{Cr}	0.3 and 0.5
	Memory size H	5

parameter settings, establishing a robust framework for fair benchmarking. The specifications of the CEC benchmarks and the performance metrics utilized are provided in Sect. 4.3. Finally, Sect. 4.4 discusses the outcomes of the comparative experiments, underscoring the superior performance of ASHADE-MPC compared to existing state-of-the-art optimization methods.

4.1 Experimental environments and implementations

Numerical experiments are conducted in the following environments.

- CPU: AMD Ryzen 5 5600X 6-Core Processor 3.70 GHz
- Memory: 32GB (2 x 16GB) DDR4
- Graphics: 8GB Nvidia GeForce RTX 4060
- Storage: 2TB NVMe M.2 PCIe SSD
- Operating system: Windows 10
- Programming language: Python 3.8

The comprehensive setup of experimental conditions and implementation strategies plays a crucial role in ensuring the replicability of this study.

4.2 Competitor algorithms and parameters

To thoroughly evaluate the performance of ASHADE-MPC in a fair and rigorous manner, we utilize 12 cutting-edge optimization algorithms as benchmark competitors, as listed below.

- State-of-the-art optimizers: DE [32], PSO [39], CMA-ES [28].
- Advanced DE variants: L-SHADE [29], jSO [30], L-SHADE-cnEpSin [31], CDE [25], CDEKI, and ISHACDE [38].
- Advanced PSO variants: Competitive Swarm Optimizer (CSO) [40], Modified CSO (MCSO) [41], and Success History Adaptive CSO with Linear Population Reduction (L-SHACSO) [42].

The parameters of these algorithms are summarized in Table 1.

Furthermore, the maximum fitness evaluation is set to 1000 multiplied by the dimension size (D), ensuring a consistent evaluation standard across all experiments. To mitigate the impact of stochasticity and enhance the reliability of our results, each algorithm is executed 50 times on a single benchmark function. This approach allows us to obtain statistically significant conclusions by reducing the

influence of random variations and ensuring robust performance assessment.

4.3 Benchmarks and performance metrics

To comprehensively analyze the performance of the proposed ASHADE-MPC, we conduct comparison experiments using three benchmark sets: CEC2017 [43], CEC2020 [44], and CEC2022 [45]. These benchmarks collectively feature a total of 51 functions, with each set containing functions that are unimodal, multimodal, hybrid, or composite. Specifically, CEC2017 includes 29 functions, CEC2020 includes 10 functions, and CEC2022 includes 12 functions. By evaluating ASHADE-MPC across these diverse benchmark sets, we aim to provide a thorough assessment of its performance under varying conditions.

To evaluate the performance of ASHADE-MPC comprehensively, we compute the mean and standard deviation (std) across 50 independent trials to demonstrate its competitive edge. To further analyze the statistical significance of ASHADE-MPC's performance relative to its competitors, we implement the Holm multiple comparison test [46]. The symbols +, ≈, and – are used to denote whether ASHADE-MPC is significantly better, not statistically different, or significantly worse than its competitors, respectively. Furthermore, the Friedman test [47] is utilized to calculate the average ranking of each optimizer, providing an additional perspective on their relative performances.

Additionally, to gain deeper insights into the balance between exploration and exploitation in ASHADE-MPC, we introduce a quantitative measure defined in Eq. (14), which helps analyze the algorithm's performance throughout the optimization process [48].

$$\begin{aligned} Div^t &= \frac{1}{D} \sum_{d=1}^D \frac{1}{N} \sum_{i=1}^N |\mathbf{x}_{mean,d}^t - \mathbf{x}_{i,d}^t| \\ Exploration &= \frac{Div^t}{Div_{max}} \\ Exploitation &= \frac{|Div^t - Div_{max}|}{Div_{max}} \end{aligned} \quad (14)$$

Here, Div^t represents the dispersion of individuals relative to the population centroid during the t^{th} iteration. This measure allows us to evaluate how effectively ASHADE-MPC balances exploration (diversification) and exploitation (intensification) during the optimization journey.

4.4 Comparison experiments and analysis

In this part, we conduct comparative experiments to assess the competitiveness of ASHADE-MPC relative to twelve

Table 2 Summarized results of comparison experiments in CEC benchmarks

Bench.	Dim.	DE	PSO	CMA-ES	L-SHADE	jSO	L-SHADE-onEpSIn	CSO	MCSO	L-SHACSO	CDE	CDEKI	ISHACDE	ASHADE-MPC
CEC2017	30	+/-/-:	29/0/0	29/0/0	21/2/6	24/3/2	28/1/0	27/1/1	14/1/14	22/1/6	13/2/14	27/2/0	15/9/5	20/8/1
		Avg. rank:	11.0	11.9	6.9	5.9	8.1	9.3	3.9	5.4	3.2	6.1	5.2	10.7
50	+/-/-:	21/1/7	26/1/2	25/1/3	28/1/0	11/5/13	17/3/9	10/3/16	26/3/0	19/5/5	18/7/4	-	-	3.2
		Avg. rank:	11.7	12.3	8.4	5.3	7.7	8.6	4.4	4.4	3.2	6.2	5.1	10.5
CEC2020	10	+/-/-:	10/0/0	10/0/0	6/2/2	7/2/1	9/1/0	8/2/0	4/3/3	9/1/0	5/4/1	5/5/0	7/3/0	8/2/0
		Avg. rank:	5/11.2	12.4	5.4	6.9	10.2	7.5	4.2	8.9	4.9	4.4	5.7	6.1
20	+/-/-:	10/0/0	10/0/0	6/0/4	8/0/2	10/0/0	10/0/0	6/0/4	9/0/1	7/0/3	8/1/1	6/4/0	5/4/1	-
		Avg. rank:	12.2	12.3	6.2	6.1	9.9	8.9	4.5	7.1	5.3	5.7	5.4	4.7
CEC2022	10	+/-/-:	9/1/2	10/0/2	9/0/3	11/0/1	12/0/0	9/0/3	10/0/2	10/1/1	9/1/2	5/5/2	7/4/1	9/3/0
		Avg. rank:	9.3	10.3	7.4	7.8	11.8	5.7	5.8	8.5	4.7	4.7	6.8	5.2
20	+/-/-:	11/0/1	11/0/1	8/1/3	10/1/1	10/0/2	8/1/3	7/1/4	7/3/2	6/1/5	10/2/0	10/0/2	7/5/0	-
		Avg. rank:	11.2	11.1	6.5	7.3	8.8	6.6	5.5	6.6	4.4	6.4	6.9	5.9

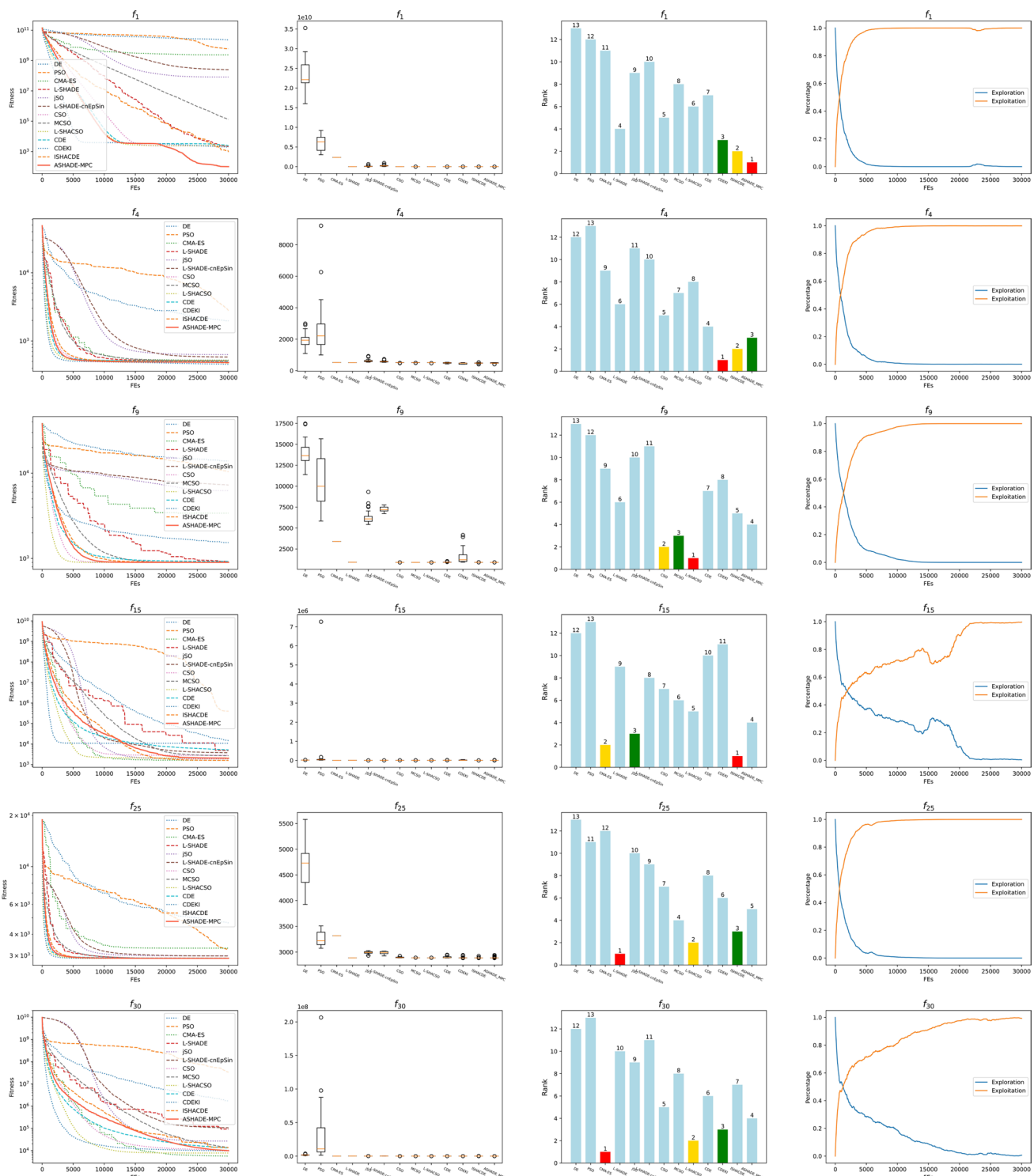


Fig. 5 Convergence curves, boxplots, ranks of optimizers, and exploration&exploitation proportions in 30-D CEC2017 representative functions

state-of-the-art optimizers. The summarized outcomes in the CEC benchmarks are tabulated in Table 2. Meanwhile, the detailed results for CEC2017, 2020, and 2022 benchmarks are respectively provided in Appendices B, C, and D. Furthermore, convergence curves, boxplots, ranks of

optimizers, and exploration&exploitation proportions of ASHADE-MPC are shown in Figs. 5, 6, 7, 8, 9, and 10.

The CEC2017, CEC2020, and CEC2022 benchmark suites, comprising unimodal, multimodal, hybrid, and composite function optimization problems, have been

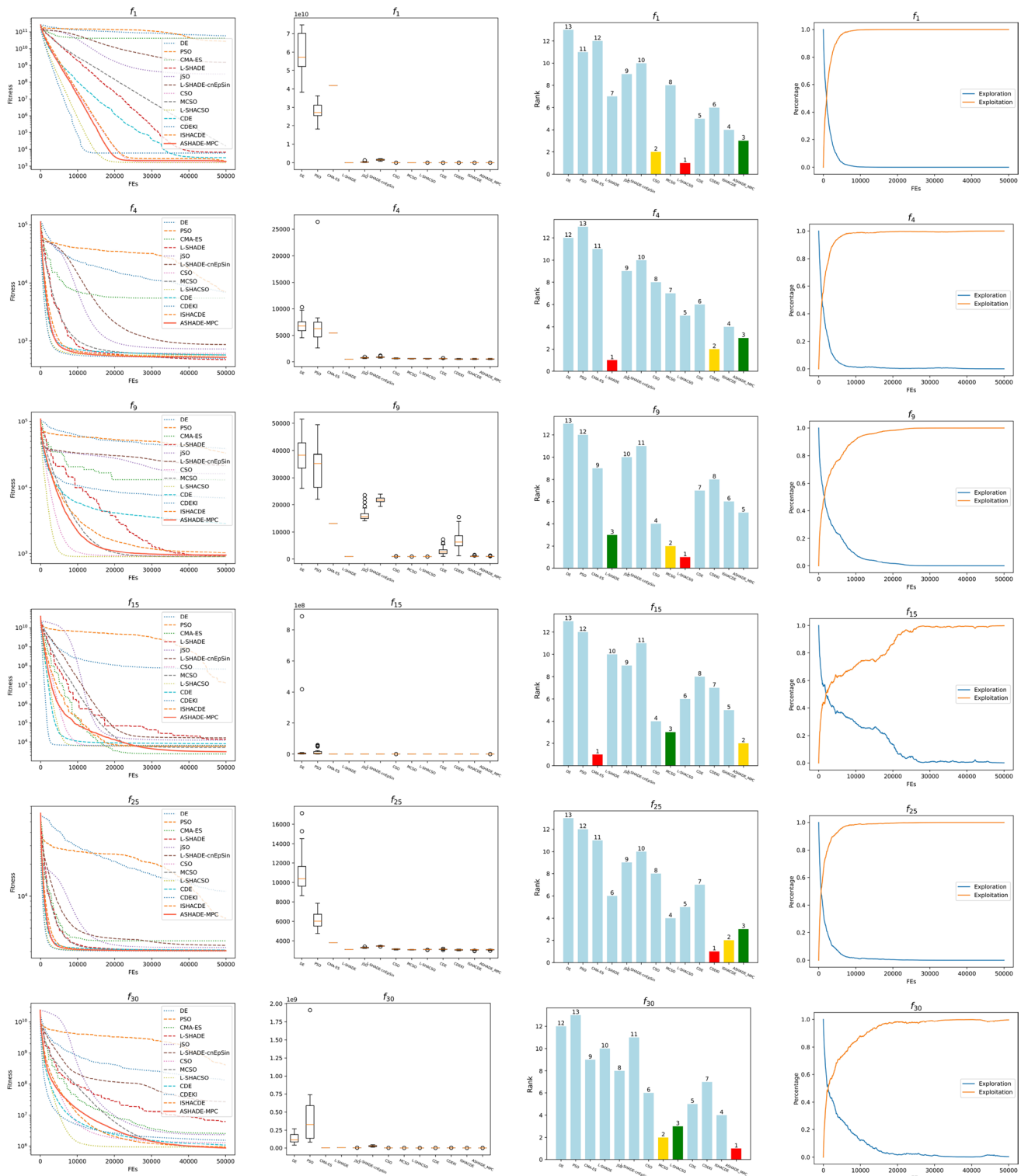


Fig. 6 Convergence curves, boxplots, ranks of optimizers, and exploration&exploitation proportions in 50-D CEC2017 representative functions

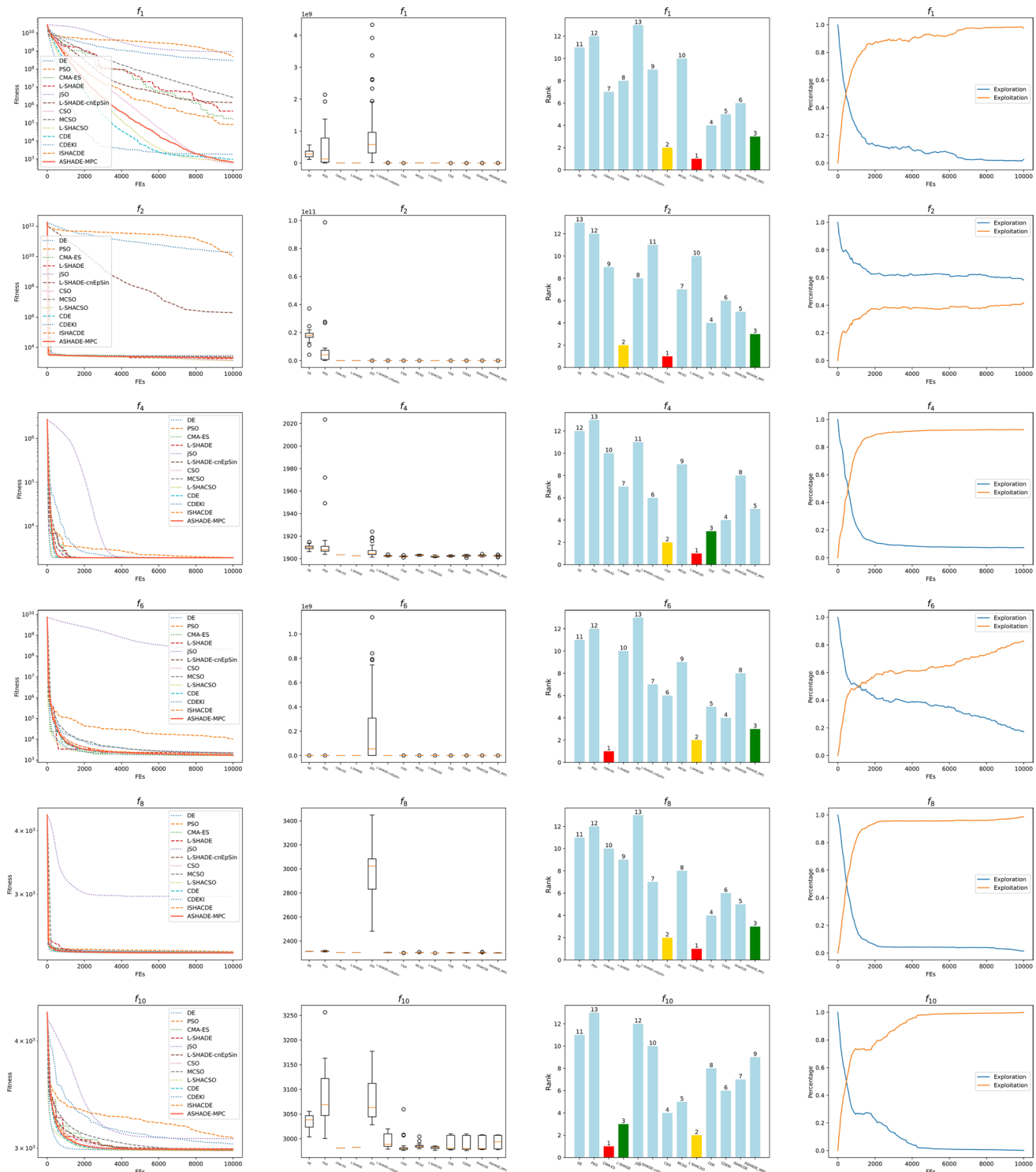


Fig. 7 Convergence curves, boxplots, ranks of optimizers, and exploration&exploitation proportions in 10-D CEC2020 representative functions

established as standard references for evaluating algorithmic robustness and scalability. Within this rigorous evaluation framework, state-of-the-art optimization algorithms were systematically selected for comparative analysis, with ASHADE-MPC undergoing comprehensive statistical

evaluation. Empirical findings demonstrate ASHADE-MPC's exceptional optimization capabilities across multiple dimensionality scales. Specifically, in the CEC2017 benchmark, the proposed algorithm demonstrates remarkable characteristics. In 30-dimensional search space, both

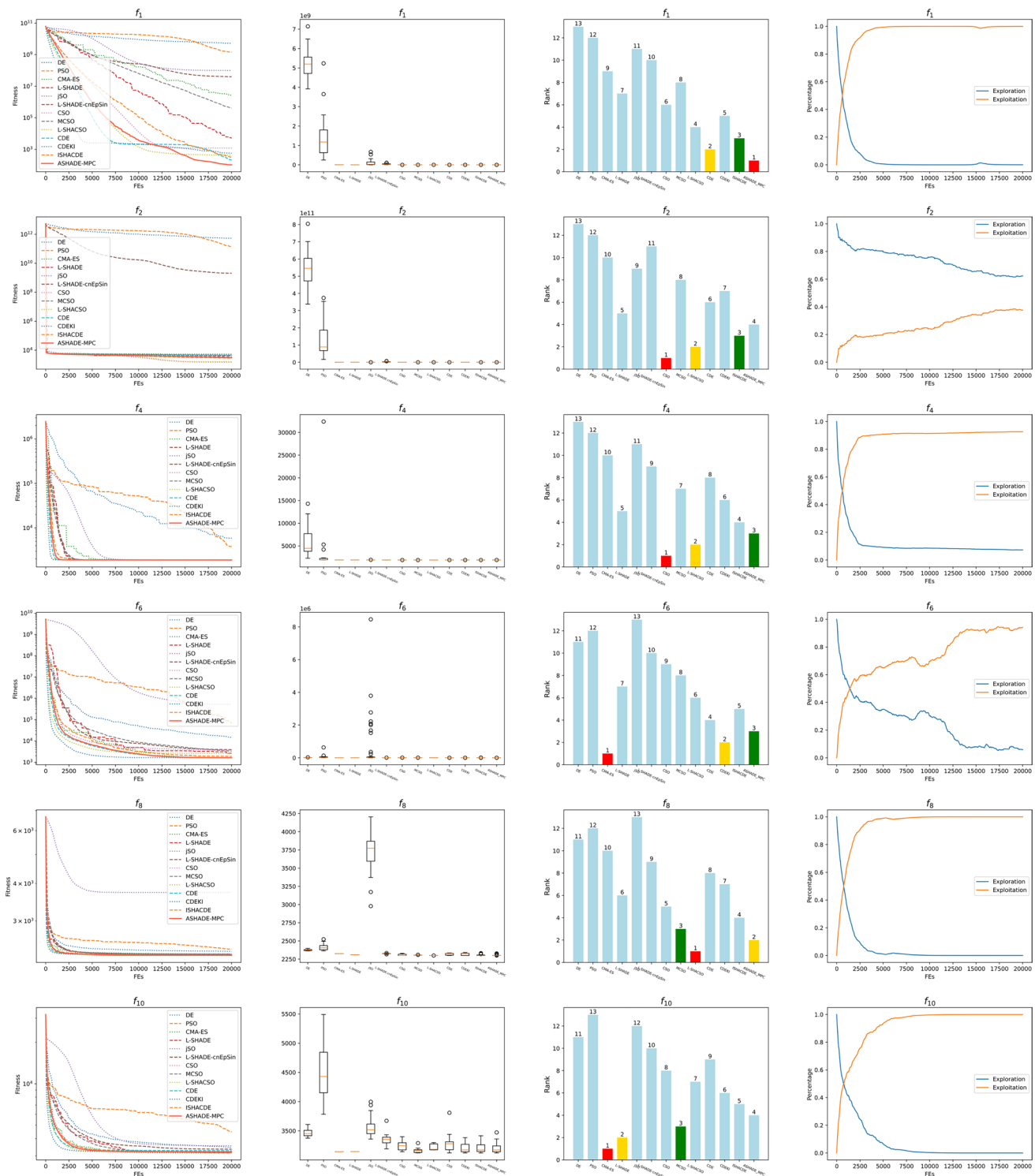


Fig. 8 Convergence curves, boxplots, ranks of optimizers, and exploration&exploitation proportions in 20-D CEC2020 representative functions

the proposed algorithm and LSHACSO shared the top position with an average ranking of 3.2. When extended to 50-dimensional space, algorithmic performance showed divergence. LSHACSO secured the first place with an average ranking of 3.2. Although exhibiting a performance gap

compared to LSHACSO in 50-dimensional space, the proposed algorithm maintained excellent stability and effectiveness throughout its optimization process, successfully claiming the second position. From the perspective of the No Free Lunch Theorem, no single algorithm can achieve

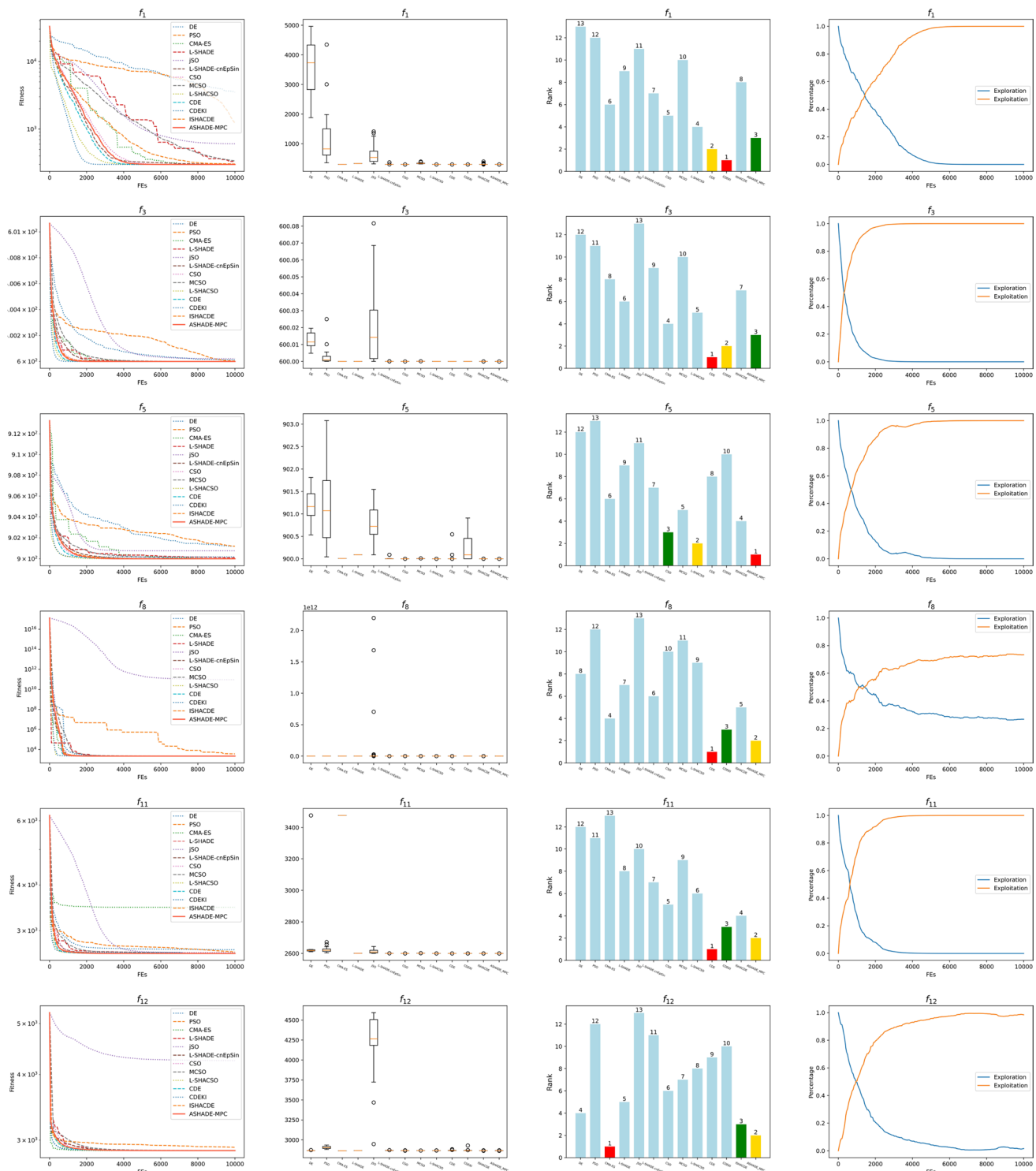


Fig. 9 Convergence curves, boxplots, ranks of optimizers, and exploration&exploitation proportions in 10-D CEC2022 representative functions

optimal performance across all problems. The second-place ranking of the proposed algorithm in 50-dimensional space does not indicate inherent flaws, but rather reflects the varying adaptability of different algorithms to distinct problem characteristics. LSHACSO's search mechanism

appears particularly aligned with the specific properties of CEC2017's 50-dimensional problems, enabling its superior performance. While slightly outperformed in this specific dimensional scenario, the proposed algorithm demonstrates capabilities to surpass LSHACSO in optimization problems

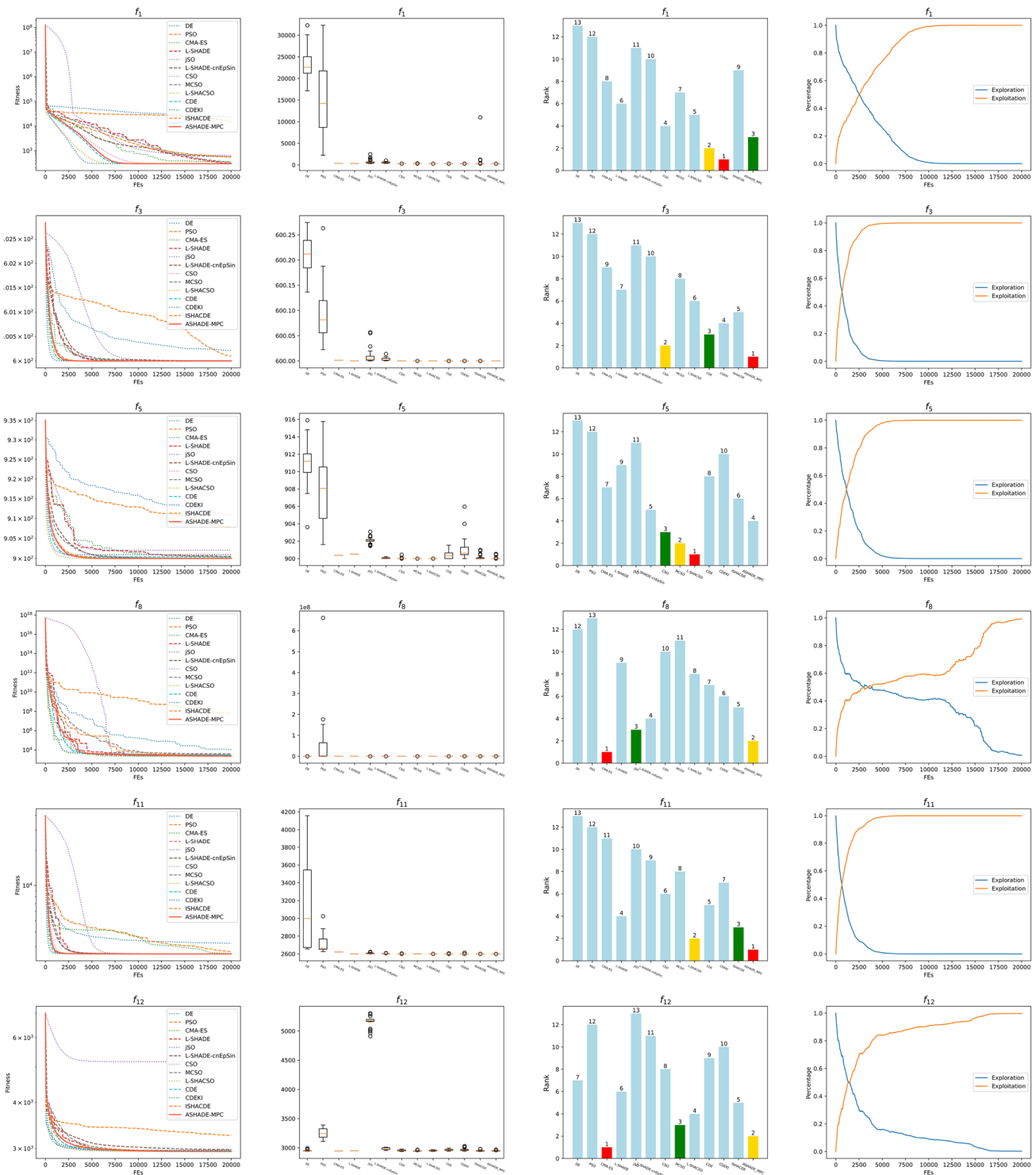


Fig. 10 Convergence curves, boxplots, ranks of optimizers, and exploration&exploitation proportions in 20-D CEC2022 representative functions

with different characteristic configurations. The algorithm maintained competitive positioning in subsequent benchmarks, achieving mean ranks of 3.2 (10-D) and 2.7 (20-D) in CEC2020, and 3.2 (10-D) with 3.7 (20-D) in CEC2022. In both CEC2020 and CEC2022, ASHADE-MPC consistently

outperformed competing algorithms, emerging as a top performer among twelve state-of-the-art algorithms.

The superior performance of ASHADE-MPC is attributed to the synergistic integration of its multi-agent participated competition mechanism and adaptive mutation probability,

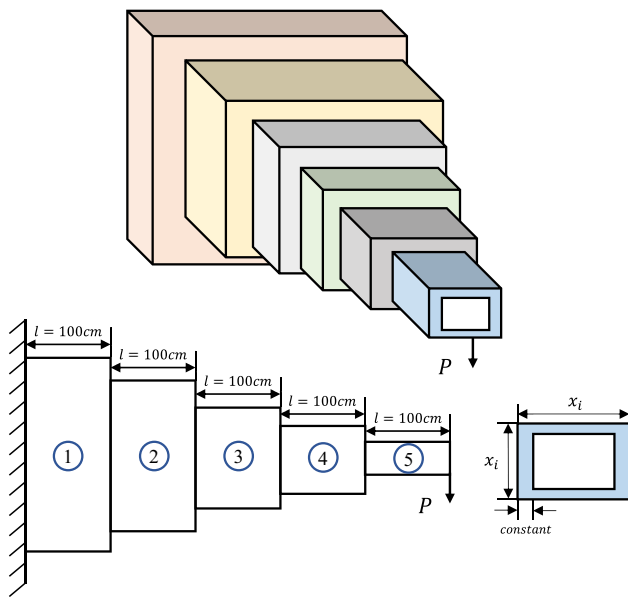


Fig. 11 The demonstration of the Cantilever Beam Design Problem

which collectively maintain dynamic equilibrium between exploration and exploitation phases. The multi-agent participated competition mechanism employs real-time fitness evaluations to dynamically select mutation operators from the DE/cur-to-mean(x_{idx1}^t, x_{idx2}^t)/1 and DE/cur-to-mean(x_{best}^t, x_{idx}^t)/1, and DE/cur-to-best/1 strategy pool, effectively mitigating premature convergence through diversified solution space exploration. This diversity preservation mechanism substantially reduces over-reliance on current elite individuals while preventing local optimum entrapment during initial optimization stages. Concurrently, the adaptive mutation probability controller incorporates the DE/best/1 operator through dynamic parameter adaptation, implementing phased search strategy adjustment: initial stages emphasize exploratory behavior through operator diversity maximization, with gradual intensification of DE/best/1 utilization as evolutionary progression occurs. This

self-adaptive transition mechanism enables seamless shifting from global exploration to local refinement, thereby preserving population diversity while progressively enhancing solution precision until convergence criteria are satisfied.

5 Numerical experiments in engineering problems

To verify the performance of the ASHADE-MPC algorithm in real-world engineering constrained optimization problems, this section compares seven engineering optimization problems from the structural domain (three-bar truss design, multi-disc clutch-brake, pressure vessel, welded beam, and gear reducer) with each other. The algorithm parameters are set according to the configuration in Table 1. For the reliability of the experimental results, all results are statistically averaged, and the maximum number of fitness evaluations for each experiment is fixed at 10,000, with each problem running independently 50 times.

5.1 Cantilever Beam Design Problem (CBDP)

The CBDP, as a classic optimization issue in the field of structural engineering, aims to design a cantilever beam structure that minimizes weight and cost while satisfying specific structural strength, stiffness, and material constraints. The manufacturing configuration of the problem is depicted in Fig. 11. Its mathematical model is described in detail in Appendix A.1. The experimental results and statistical analysis are summarized in Table 3. Furthermore, to visually demonstrate the optimization process and outcomes, Fig. 12 shows the convergence curve of the optimization algorithm, boxplots, and the ranking of optimizers.

Table 3 Results of optimizers in CBDP

MAs	Mean	std	Best	Worst
DE	3.13192e+00 +	4.46100e-01	2.40066e+00	4.23036e+00
PSO	2.19392e+00 +	3.52426e-01	1.67011e+00	2.78357e+00
CMA-ES	1.34241e+00 +	1.07599e-03	1.34031e+00	1.34497e+00
L-SHADE	2.06585e+00 +	3.10591e-01	1.46328e+00	3.08039e+00
jSO	2.62436e+00 +	4.15014e-01	1.90377e+00	3.30754e+00
L-SHADE-cnEpSin	1.34455e+00 +	2.09161e-03	1.34169e+00	1.34961e+00
CSO	1.34253e+00 +	1.17221e-03	1.34054e+00	1.34549e+00
MCSO	1.34020e+00 +	1.85265e-04	1.34003e+00	1.34118e+00
L-SHACSO	1.34189e+00 +	1.41684e-03	1.34012e+00	1.34757e+00
CDE	1.34020e+00 -	1.85265e-04	1.34003e+00	1.34118e+00
CDEKI	1.34095e+00 +	3.56314e-04	1.34052e+00	1.34178e+00
ISHACDE	1.34012e+00 -	3.42153e-04	1.33997e+00	1.34242e+00
ASHADE-MPC	1.34025e+00	1.40588e-04	1.34003e+00	1.34057e+00

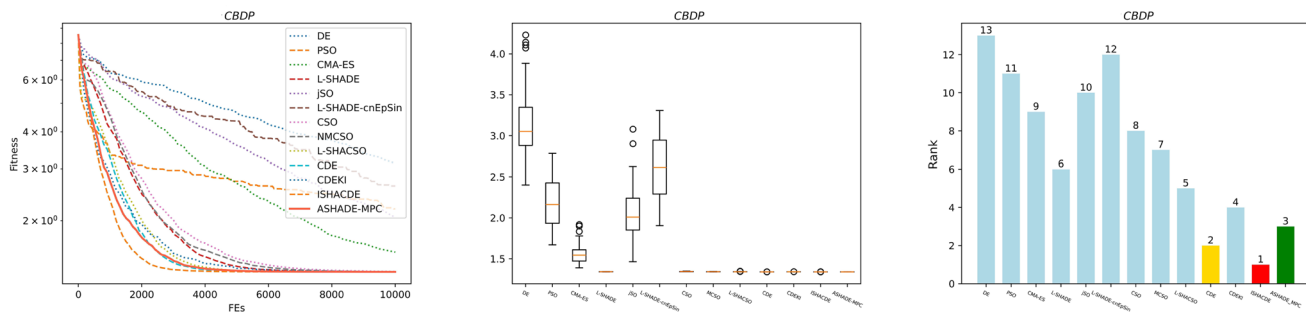


Fig. 12 Convergence curves, boxplots, and ranks of optimizers in Cantilever Beam Design Problem

Table 4 Results of optimizers in CBHDP

MA	mean	std	best	worst
DE	7.20843e+00	1.32935e-01	6.96257e+00	7.78961e+00
PSO	7.47412e+00	2.50550e-01	7.14962e+00	8.00434e+00
CMA-ES	6.86007e+00	8.86971e-03	6.84757e+00	6.88270e+00
L-SHADE	6.95609e+00	4.00149e-02	6.88013e+00	7.08521e+00
jSO	6.98068e+00	6.04585e-02	6.86339e+00	7.11020e+00
L-SHADE-cnEpSin	6.86051e+00	7.32901e-03	6.84557e+00	6.88169e+00
CSO	6.85511e+00	3.26985e-03	6.84684e+00	6.86279e+00
MCSO	6.84372e+00	7.02864e-04	6.84309e+00	6.84657e+00
L-SHACSO	6.84832e+00	2.60540e-03	6.84443e+00	6.85488e+00
CDE	6.84372e+00	7.02864e-04	6.84309e+00	6.84657e+00
CDEKI	6.84818e+00	1.09739e-03	6.84637e+00	6.84931e+00
ISHACDE	6.84324e+00	5.51748e-04	6.84297e+00	6.84586e+00
ASHADE-MPC	6.84371e+00	5.49864e-04	6.84308e+00	6.84579e+00

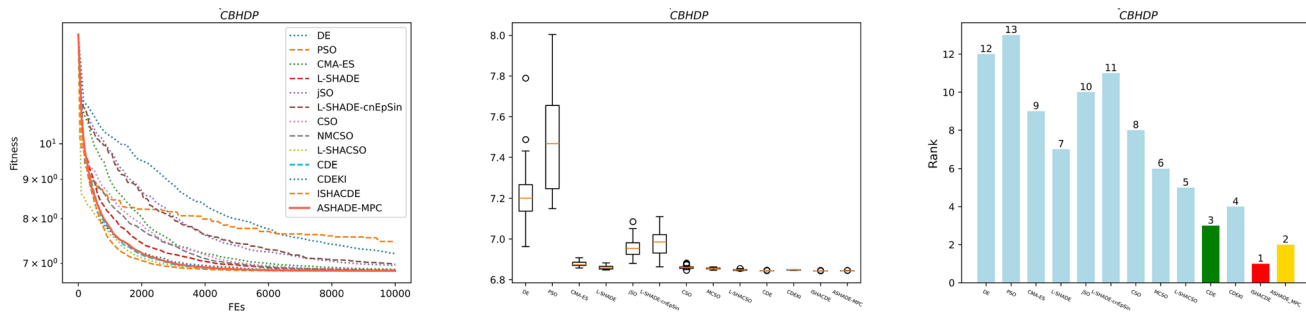


Fig. 13 Ranks, convergence curves, and boxplots of optimizers in CBHDP

5.2 Corrugated Bulkhead Design Problem (CBHDP)

The CBHDP focuses on optimizing the design of bulkheads, commonly used in ships and large structures, to enhance strength, stiffness, and stability. The objective is to reduce costs while ensuring that performance constraints, such as strength, deflection, and buckling, are satisfied. The mathematical model is detailed in Appendix A.2, with results summarized in Table 4 and optimizer performance shown in Fig. 13. The Corrugated Bulkhead Design Problem (CBHDP) is an important optimization problem in the field of ship and ocean engineering. Its core objective is to optimize the design of bulkhead structures to enhance their strength, stiffness, and stability, while minimizing costs

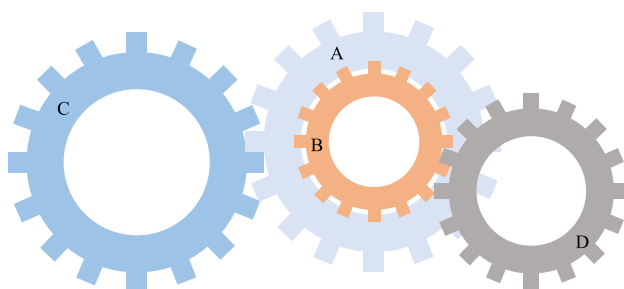
as much as possible. The Corrugated Bulkhead Design Problem can be transformed into a complex nonlinear optimization problem through mathematical modeling. Its mathematical model is described in detail in Appendix A.2. The experimental results and statistical analysis are summarized in Table 4, and Fig. 13 shows the convergence curve of the optimization algorithm, boxplots, and the ranking of optimizers.

5.3 Gear Train Design Problem (GTDP)

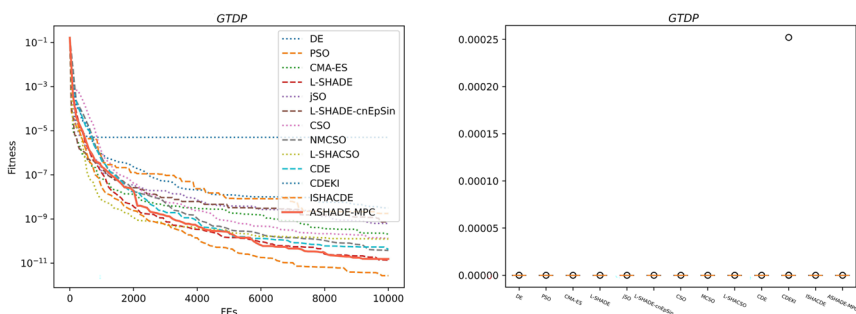
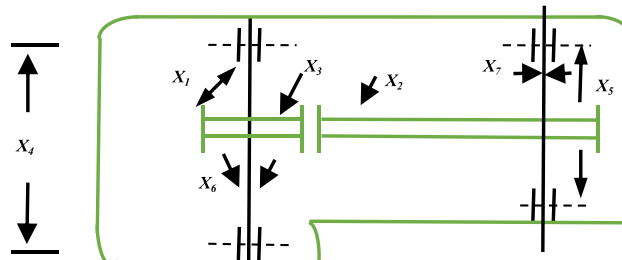
The GTDP is an optimization task in mechanical engineering aimed at designing a gear train to obtain a particular gear ratio while maintaining efficient power transmission and

Table 5 Results of optimizers in GTDP

MAs	mean	std	best	worst
DE	3.19284e-09	9.66511e-09	1.97632e-13	6.40810e-08
PSO	1.77559e-09	3.71365e-09	1.84302e-12	1.64131e-08
CMA-ES	1.36990e-11	2.26938e-11	1.85613e-15	1.04472e-10
L-SHADE	6.27841e-10	1.67643e-09	1.78088e-13	1.17198e-08
jSO	7.35969e-10	1.02616e-09	6.94476e-12	4.19842e-09
L-SHADE-cnEpSin	1.34869e-10	2.82961e-10	7.50956e-14	1.84930e-09
CSO	3.78106e-11	6.73690e-11	5.29430e-15	3.68503e-10
MCSO	4.18144e-11	1.15234e-10	1.94605e-15	7.57464e-10
L-SHACSO	1.25279e-10	2.15350e-10	7.07669e-14	1.03004e-09
CDE	4.18144e-11	1.15234e-10	1.94605e-15	7.57464e-10
CDEKI	5.04709e-05	3.52996e-05	4.23031e-24	2.52144e-04
ISHACDE	2.71000e-12	1.35880e-11	2.28845e-24	9.40445e-11
ASHADE-MPC	1.54214e-11	9.12514e-11	3.76599e-18	6.52798e-10

**Fig. 14** The demonstration of the Gear Train Design Problem

reliability. The mathematical formulation of GTDP is available in Appendix A.3, with results summarized in Table 5, and Fig. 14 illustrates the optimizer rankings, convergence plots, and boxplots.

**Fig. 15** Ranks, convergence curves, and boxplots of optimizers in GTDP**Fig. 16** The demonstration of the Speed Reducer Design Problem

The GTDP is a classic optimization problem, with the main goal being to design a gear system to achieve a predetermined gear ratio while ensuring efficient power transmission and long-term system reliability. The solution to such problems typically requires a comprehensive consideration of multiple factors, including the size, shape, material, and manufacturing process of the gears. The mathematical model of GTDP (Gear Train Design Problem) details these design objectives and constraints. The manufacturing configuration of the problem is depicted in Fig. 14. For specific content please refer to Appendix A.3. The experimental results are summarized in Table 5, while Fig. 15 shows the rankings of the optimizer in different experiments, the convergence process, and the boxplots of performance, providing a visual analysis for comparing the performance of different optimization algorithms.

5.4 Speed Reducer Design Problem (SRDP)

The SRDP is an important optimization problem in the field of mechanical engineering. Its core objective is to design a speed reducer that increases the output torque while reducing the input speed of the motor to the desired output speed. By optimizing the design of the speed reducer, manufacturing costs are reduced. The manufacturing configuration of the problem is depicted in Fig. 16. Appendix A.5 outlines the mathematical model of SRDP, Table 6 summarizes the results, and Fig. 17 illustrates the optimizer rankings, convergence graphs, and boxplots.

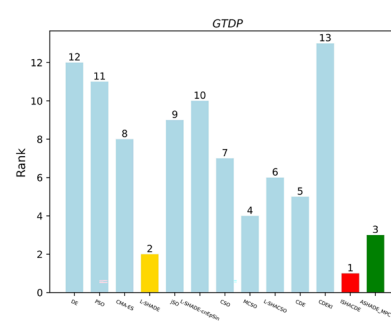
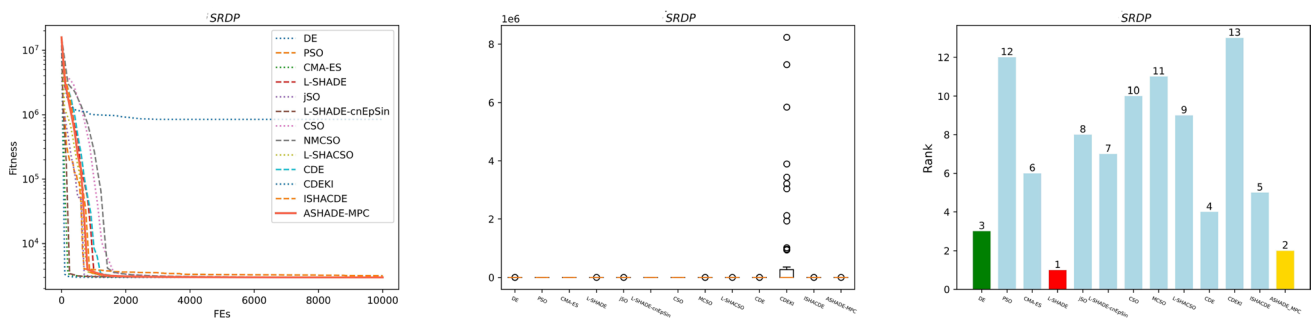
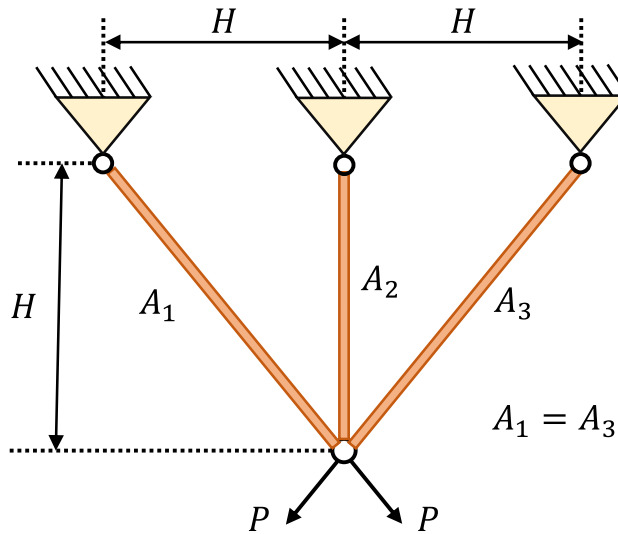


Table 6 Results of optimizers in SRDP

MAs	mean	std	best	worst
DE	2.98781e+03	3.78016e+00	2.98688e+03	3.00426e+03
PSO	3.16702e+03	5.62145e+01	3.04938e+03	3.29992e+03
CMA-ES	2.98707e+03	7.46465e-02	2.98694e+03	2.98723e+03
L-SHADE	2.99344e+03	4.65341e+00	2.98816e+03	3.00625e+03
jSO	2.99318e+03	1.89364e+00	2.99013e+03	2.99651e+03
L-SHADE-cnEpSin	2.99500e+03	2.51658e+00	2.98943e+03	3.00074e+03
CSO	2.99587e+03	2.40825e+00	2.99244e+03	3.00532e+03
MCSO	2.98791e+03	9.93634e-01	2.98713e+03	2.99205e+03
L-SHACSO	2.99349e+03	2.75673e+00	2.98909e+03	3.00517e+03
CDE	2.98791e+03	9.93634e-01	2.98713e+03	2.99205e+03
CDEKI	8.48870e+05	1.88093e+06	3.00181e+03	8.23266e+06
ISHACDE	2.98887e+03	4.77673e+00	2.98714e+03	3.01298e+03
ASHADE-MPC	2.98742e+03	2.15096e-01	2.98712e+03	2.98797e+03

**Fig. 17** Ranks, convergence curves, and boxplots of optimizers in SRDP**Fig. 18** The demonstration of the Three Bar Truss Design Problem

5.5 Three Bar Truss Design Problem (TBTDP)

The TBTDP is a common issue in the field of structural engineering. The problem primarily focuses on designing a truss system composed of three bars, with the core objective of minimizing the overall weight as much as possible while ensuring that the structure can safely support the

predetermined loads, with constraints being stress, deflection, and buckling. The manufacturing configuration of the problem is depicted in Fig. 18. Appendix A.5 outlines the mathematical model of TBTDP, Table 7 summarizes the results, and Fig. 19 illustrates the optimizer rankings, convergence graphs, and boxplots.

5.6 Tubular Column Design Problem (TCDP)

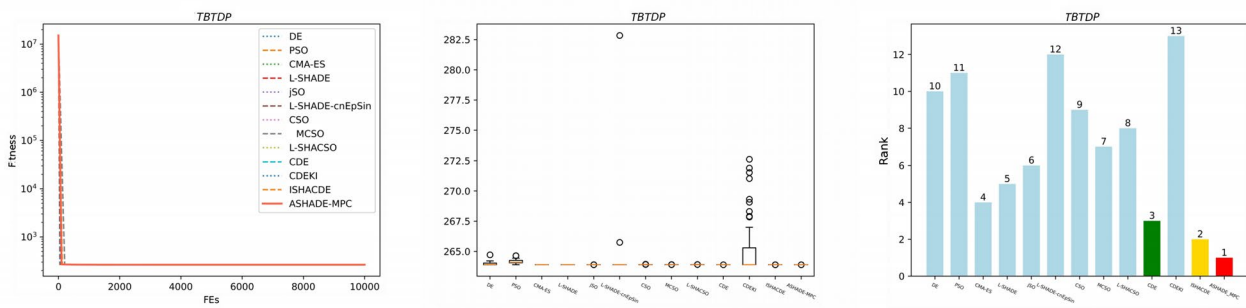
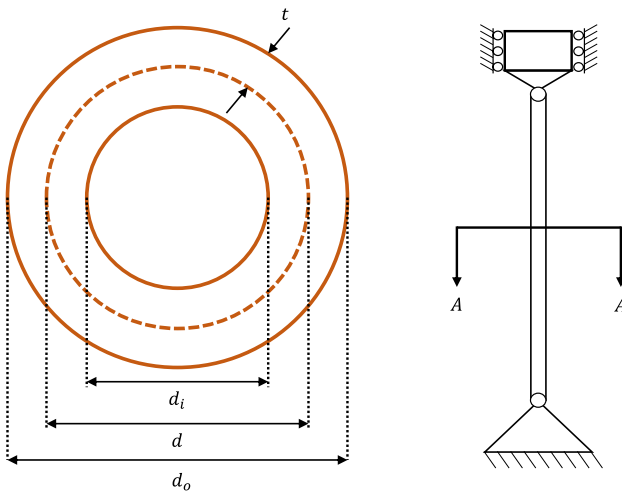
The TCDP represents a significant challenge in structural engineering, focusing on the creation of a hollow cylindrical column that can sustain given loads while striving for weight reduction. Key design parameters for such columns typically encompass the outer diameter, thickness, and length. The manufacturing configuration of the problem is depicted in Fig. 20. The detailed mathematical model of TCDP is presented in Appendix A.6, and the results are compiled in Table 8. Table 8 summarizes the results, and Fig. 21 illustrates the optimizer rankings, convergence graphs, and boxplots.

5.7 Welded Beam Design Problem (WBDP)

The WBDP is a critical optimization task in the field of structural engineering, with the core objective of minimizing the total manufacturing cost of the beam while ensuring

Table 7 Results of optimizers in TBTDP

MAs	mean	std	best	worst
DE	2.64007e+02 +	1.91981e-01	2.63896e+02	2.64712e+02
PSO	2.64174e+02 +	2.07303e-01	2.63897e+02	2.64649e+02
CMA-ES	2.63896e+02 +	2.88565e-05	2.63896e+02	2.63896e+02
L-SHADE	2.63896e+02 +	1.04939e-03	2.63896e+02	2.63901e+02
jSO	2.64936e+02 +	4.12785e+00	2.63896e+02	2.82843e+02
L-SHADE-cnEpSin	2.63904e+02 +	6.98315e-03	2.63896e+02	2.63938e+02
CSO	2.63900e+02 +	3.94018e-03	2.63896e+02	2.63912e+02
MCSO	2.63896e+02 +	1.99170e-07	2.63896e+02	2.63896e+02
L-SHACSO	2.63900e+02 +	4.38234e-03	2.63896e+02	2.63918e+02
CDE	2.63896e+02 +	1.99170e-07	2.63896e+02	2.63896e+02
CDEKI	2.65192e+02 +	2.43904e+00	2.63896e+02	2.72622e+02
ISHACDE	2.63896e+02 +	1.03718e-06	2.63896e+02	2.63896e+02
ASHADE-MPC	2.63896e+02	2.83417e-08	2.63896e+02	2.63896e+02

**Fig. 19** Ranks, convergence curves, and boxplots of optimizers in TBTDP**Fig. 20** The demonstration of the Tubular Column Design Problem

that it can withstand the applied loads under specified constraints. The manufacturing configuration of the problem is depicted in Fig. 22. The mathematical model of WBDP is detailed in Appendix A.7., Table 9 summarizes the results, and Fig. 23 illustrates the optimizer rankings, convergence graphs, and boxplots.

We have tallied the average ranking of the proposed ASHADE-MPC in practical engineering optimization

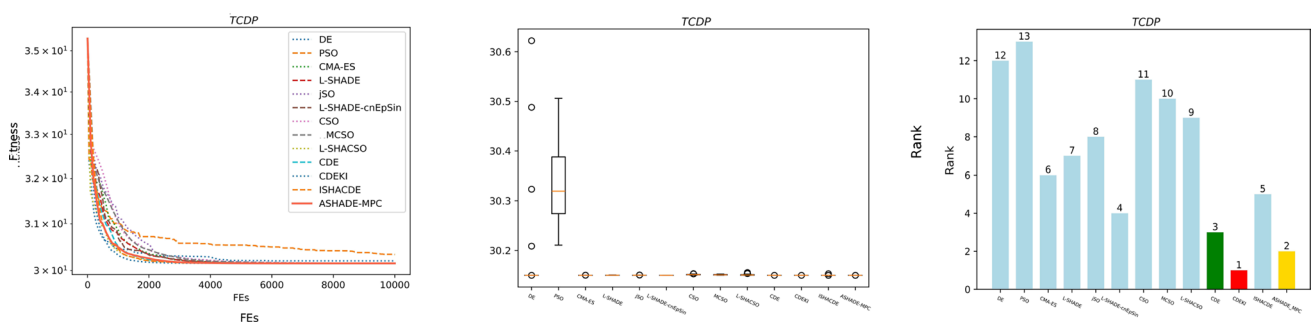
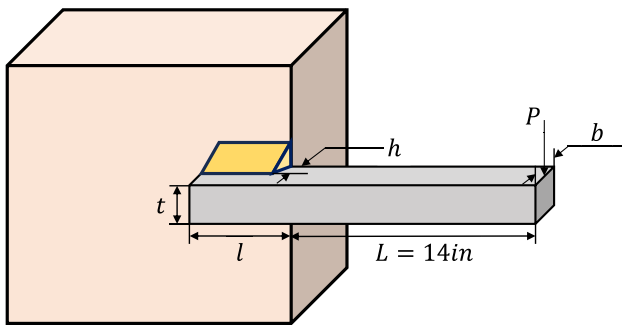
problems, and from Fig. 24, it can be observed that ASHADE-MPC achieved the first place in overall ranking. Notably, ASHADE-MPC performed exceptionally well in most cases, securing a top-three ranking in seven engineering optimization problems, maintaining statistical comparability. This further validates the effectiveness and competitiveness of ASHADE-MPC, especially its higher robustness in constrained optimization problems, demonstrating the broad application prospects of ASHADE-MPC in addressing complex engineering optimization challenges.

6 Application in coffee leaf disease detection

As a globally consumed commodity with annual production exceeding 10 million tons, coffee traces its origins to the Ethiopian highlands and is predominantly cultivated within the "Coffee Belt" between 25°N and 25°S latitude, where ideal climatic conditions prevail. The coffee industry now serves as a vital economic pillar for numerous countries. However, climate change has led to increased incidence of foliar diseases in traditional growing regions, particularly coffee leaf rust, which significantly impacts yields [49, 50].

Table 8 Results of optimizers in TCDP

MAs	mean	std	best	worst
DE	3.02019e+01 +	1.25903e-01	3.01497e+01	3.06224e+01
PSO	3.03374e+01 +	8.46544e-02	3.02107e+01	3.05061e+01
CMA-ES	3.01499e+01 +	1.37729e-04	3.01498e+01	3.01502e+01
L-SHADE	3.01499e+01 +	1.62375e-04	3.01497e+01	3.01504e+01
jSO	3.01498e+01 +	2.10286e-05	3.01497e+01	3.01498e+01
L-SHADE-cnEpSin	3.01510e+01 +	6.47128e-04	3.01499e+01	3.01531e+01
CSO	3.01507e+01 +	5.46942e-04	3.01499e+01	3.01521e+01
MCSO	3.01497e+01 +	1.30108e-06	3.01497e+01	3.01497e+01
L-SHACSO	3.01507e+01 +	1.02225e-03	3.01498e+01	3.01553e+01
CDE	3.01497e+01 +	1.30108e-06	3.01497e+01	3.01497e+01
CDEKI	3.01497e+01 -	2.91171e-08	3.01497e+01	3.01497e+01
ISHACDE	3.01498e+01 +	4.56419e-04	3.01497e+01	3.01530e+01
ASHADE-MPC	3.01497e+01	7.27061e-07	3.01497e+01	3.01497e+01

**Fig. 21** The demonstration of the Tubular Column Design Problem**Fig. 22** The demonstration of the Welded Beam Design Problem

Recent advancements in deep learning have shifted disease detection from visual inspection to deep learning-based solutions. While significant progress has been made in developing precise and adaptable models under controlled conditions, practical applications face multiple challenges. Environmental variability, data discrepancies from imaging equipment differences, and insufficient annotated data collectively constrain model performance. Specifically, environmental fluctuations may cause data distribution shifts that compromise generalization capabilities, imaging device variations introduce additional data bias, and data scarcity limits models' ability to learn real-world complexities, resulting in suboptimal performance on unseen data. Addressing these issues requires innovative methodologies

to enhance model effectiveness and reliability in diverse environments.

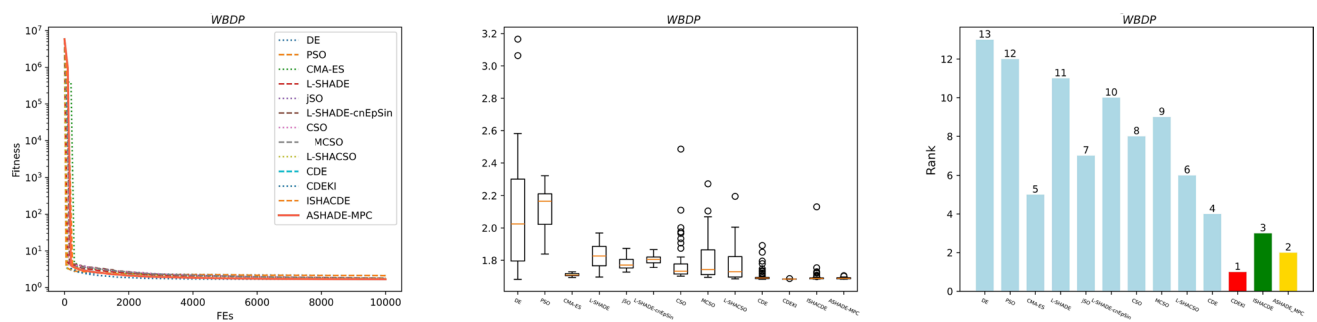
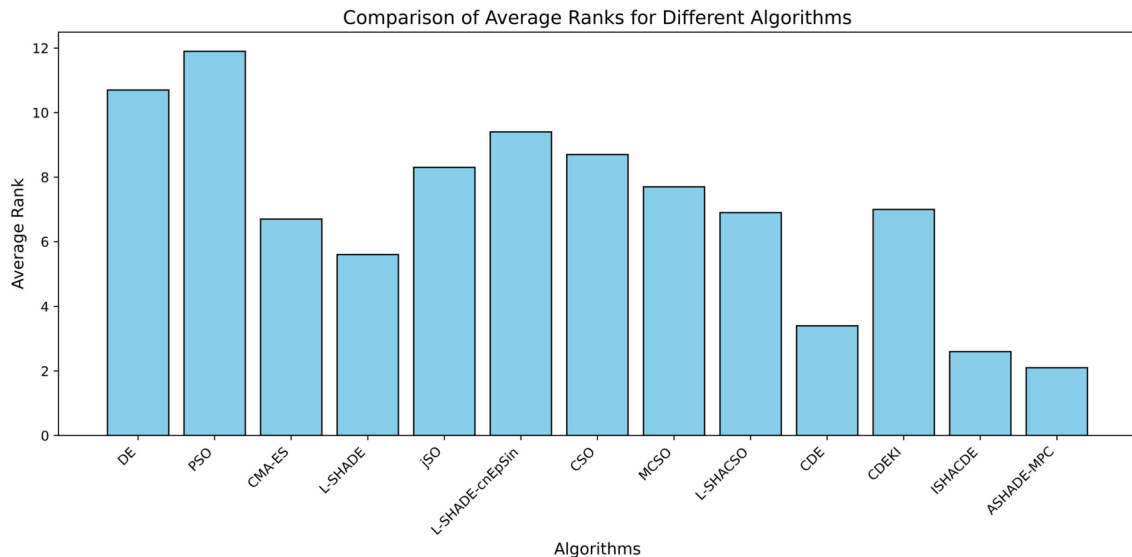
To address these challenges, this study proposes an ASHADE-MPC-optimized ensemble learning framework (ASHADE-MPC-Ensemble). The framework employs multiple ImageNet-pretrained deep neural networks fine-tuned on coffee leaf disease datasets, selecting three top-performing models. These are subsequently integrated through an ASHADE-MPC-optimized soft voting mechanism to enhance overall accuracy and robustness. Section 6.1 details the architectural design, Sect. 6.2 specifies experimental parameters and dataset configuration, while Sect. 6.3 presents comparative experiments demonstrating enhanced diagnostic effectiveness in intelligent coffee disease detection.

6.1 The architecture of ASHADE-MPC-Ensemble

This section presents the architecture of the proposed ASHADE-MPC-Ensemble model, as shown in Fig. 25. The proposed model begins with fine-tuning eight pre-trained deep learning models in the coffee leaf disease dataset to utilize the ability of feature extraction and improve task-specific accuracy. After the evaluation based on the classification performance, the top three with the highest accuracies are selected for inclusion in the ensemble. The

Table 9 Results of optimizers in WBDP

MAs	mean	std	best	worst
DE	2.12921e+00 +	4.24338e-01	1.68257e+00	3.16562e+00
PSO	2.12058e+00 +	1.34369e-01	1.83917e+00	2.32265e+00
CMA-ES	1.81785e+00 +	7.15566e-02	1.69665e+00	1.96849e+00
L-SHADE	1.77779e+00 +	3.78753e-02	1.72726e+00	1.87394e+00
jSO	1.80392e+00 +	2.86576e-02	1.75555e+00	1.86595e+00
L-SHADE-cnEpSin	1.78290e+00 +	1.33989e-01	1.70194e+00	2.48579e+00
CSO	1.79847e+00 +	1.27922e-01	1.69514e+00	2.27324e+00
MCSO	1.70516e+00 +	4.10113e-02	1.68321e+00	1.89221e+00
L-SHACSO	1.76888e+00 +	9.87456e-02	1.68538e+00	2.19546e+00
CDE	1.70516e+00 +	4.10113e-02	1.68321e+00	1.89221e+00
CDEKI	1.68430e+00 -	8.69401e-04	1.68285e+00	1.68726e+00
ISHACDE	1.70154e+00 +	6.28813e-02	1.68419e+00	2.13118e+00
ASHADE-MPC	1.69007e+00	5.18175e-03	1.68393e+00	1.70578e+00

**Fig. 23** Ranks, convergence curves, and boxplots of optimizers in WBDP**Fig. 24** Comparison of Average Ranks for Different Algorithms

selected models are integrated using a soft voting scheme, which combines the predictions by assigning weights to each model. Unlike traditional fixed-weight ensembles, the weights in ASHADE-MPC-Ensemble are dynamically and iteratively optimized using the proposed ASHADE-MPC. Finally, the optimized ensemble model performs disease

prediction, which integrates the complementary strengths of the selected deep learning models to achieve superior accuracy and robustness in detecting coffee leaf diseases.

To combine the predictions from these top models, a soft voting strategy is adopted. In this approach, each model's influence on the final ensemble decision is controlled by a

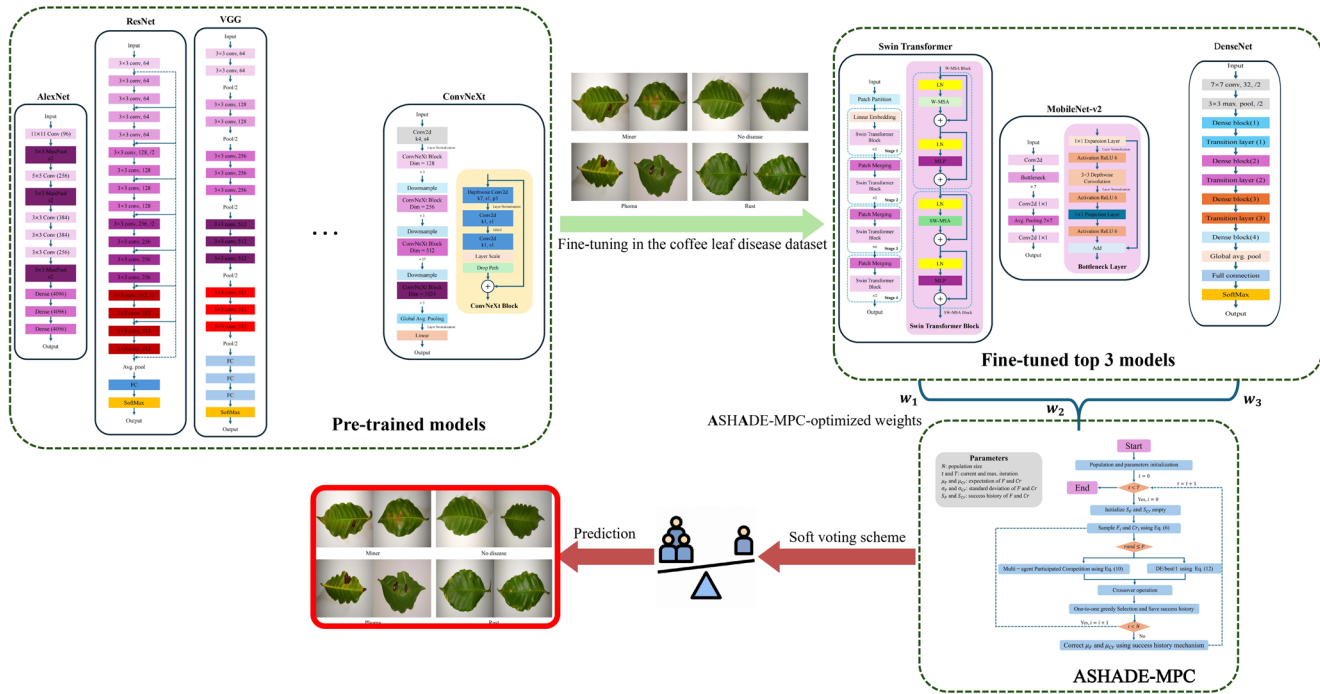


Fig. 25 The architecture of ASHADE-MPC-Ensemble

set of weighting coefficients, represented as \mathbf{w}_1 , \mathbf{w}_2 , and \mathbf{w}_3 . These coefficients reflect the relative importance of each model's predictions, where better-performing models receive higher weights. The optimization of these weights is performed using the ASHADE-MPC algorithm, which is specifically designed to adjust these coefficients for optimal ensemble performance. The ASHADE-MPC algorithm effectively balances the contributions of individual models, enabling the ensemble to leverage the strengths of each model while mitigating their weaknesses.

The evaluation function for soft voting within ASHADE-MPC is defined by Equation (15). The complete pseudocode of the ASHADE-MPC-Ensemble approach is provided in Algorithm 2.

Notation System:

- $\mathbf{x} \in \mathbb{R}^d$: Input feature vector with dimension d
- $y \in \{1, \dots, C\}$: Ground-truth class label for \mathbf{x}
- $\mathcal{D}_{\text{val}} = \{(\mathbf{x}^{(1)}, y^{(1)}), \dots, (\mathbf{x}^{(m)}, y^{(m)})\}$: Validation set with m samples
- $p_{kc}^{(x)}$: Probability of class c from model k for sample \mathbf{x}
- $\mathbf{p}_k^{(x)} \in [0, 1]^C$: Probability distribution vector from model k
- $\mathbf{p}_{\text{ens}}^{(x)} \in [0, 1]^C$: Ensemble probability vector
- $w_{i,k}^t \in [0, 1]$: Weight for model k in individual i at generation t
- C : Number of classes, N : Population size
- $\mathbb{I}(\cdot)$: Indicator function (1 if correct prediction, 0 otherwise)
- $f_k(\cdot)$: Base model k producing probability distributions
- $\arg \max_c$: Index of maximum probability component

$$f(\mathbf{w}_i^t) = \frac{1}{|\mathcal{D}_{\text{val}}|} \sum_{(\mathbf{x}, y) \in \mathcal{D}_{\text{val}}} \mathbb{I}\left(y = \arg \max_c [\mathbf{p}_{\text{ens}}^{(x)}]_c\right)$$

where $[\mathbf{p}_{\text{ens}}^{(x)}]_c = \sum_{k=1}^3 w_{i,k}^t p_{kc}^{(x)}$ (Ensemble probability)

$$\mathbf{p}_k^{(x)} = \begin{bmatrix} p_{k1}^{(x)} \\ \vdots \\ p_{kC}^{(x)} \end{bmatrix} = f_k(\mathbf{x}) \quad (\text{Base model output}) \quad (15)$$

$p_{kc}^{(x)} \in [0, 1]$ (Class probability)

$$\sum_{c=1}^C p_{kc}^{(x)} = 1 \quad (\text{Probability constraints})$$



Input: Training data: $\mathcal{D}_{\text{train}}$,
 Validation data: \mathcal{D}_{val} ,
 Base models: $\{M_1, M_2, M_3\}$,
 ASHADE-MPC parameters: N, FE_{\max}

Output: Optimal weights: $\mathbf{w}^* = (\omega_1, \omega_2, \omega_3)$

```

1 Function ASHADE-MPC-Ensemble ( $\mathcal{D}_{\text{train}}, \mathcal{D}_{\text{val}}, \{M_1, M_2, M_3\}, N, FE_{\max}\$ ):
2   Train base models on  $\mathcal{D}_{\text{train}}$ 
3   Initialize population of weight vectors  $\{\mathbf{w}_i\}_{i=1}^N$  where  $\sum_{k=1}^3 \omega_k = 1$ 
4    $t = 0, FE = 0$ 
5   Record best weight  $\mathbf{w}_{\text{best}}^t$ 
6   while  $FE < FE_{\max}$  do
7     Initialize success history memory
8     Sample  $\mu_{F,r}$  and  $\mu_{Cr,r}$  from historical memory
9     Generate adaptive probability  $P$  via formula (10)
10    for  $i = 0$  to  $N$  do
11      Randomly sample distinct indices  $idx1, idx2, r1, r2 \in \{0, 1, \dots, N - 1\} \setminus \{i\}$ 
12      if  $rand < P$  then
13        if  $f(\mathbf{w}_i^t) > \max(f(\mathbf{w}_{idx1}^t), f(\mathbf{w}_{idx2}^t))$  then
14           $\mathbf{v}_i^t = \mathbf{w}_i^t + F \left( \text{mean}(\mathbf{w}_{idx1}^t, \mathbf{w}_{idx2}^t) - \mathbf{w}_i^t \right) + F_1 \times (\mathbf{w}_{r1}^t - \mathbf{w}_{r2}^t)$ 
15        end
16        else if  $f(\mathbf{w}_i^t) < \min(f(\mathbf{w}_{idx1}^t), f(\mathbf{w}_{idx2}^t))$  then
17           $\mathbf{v}_i^t = \mathbf{w}_i^t + F_1 \times (\mathbf{w}_{\text{best}}^t - \mathbf{w}_i^t) + F_1 \times (\mathbf{w}_{r1}^t - \mathbf{w}_{r2}^t)$ 
18        end
19        else
20          Randomly select an index from  $idx1$  and  $idx2$  and assign it to  $idx$ 
21           $\mathbf{v}_i^t = \mathbf{w}_i^t + F \left( \text{mean}(\mathbf{w}_{\text{best}}^t, \mathbf{w}_{idx}^t) - \mathbf{w}_i^t \right) + F_1 \times (\mathbf{w}_{r1}^t - \mathbf{w}_{r2}^t)$ 
22        end
23      end
24      else
25         $\mathbf{v}_i^t = \mathbf{w}_{\text{best}}^t + F \times (\mathbf{w}_{r1}^t - \mathbf{w}_{r2}^t)$ 
26      end
27      Perform binomial crossover between  $\mathbf{v}_i^t$  and  $\mathbf{w}_i^t$ 
28      Project  $\mathbf{v}_i^t$  to simplex space ( $\sum \omega_k = 1$ )
29      Clip weights to [0,1]
30      Evaluate ensemble accuracy on  $\mathcal{D}_{\text{val}}$  via formula (15)
31      Update  $FE \leftarrow FE + 1$ 
32      Update historical memory using the SHA mechanism
33    end
34    Update  $\mathbf{w}_{\text{best}}^t$ 
35     $t \leftarrow t + 1$ 
36  end
37  return  $\mathbf{w}_{\text{best}}^t$ 

```

Algorithm 2 ASHADE-MPC-Ensemble

6.2 Experimental settings and datasets

This section describes the experimental setup and dataset. In the ASHADE-MPC-Ensemble algorithm parameters, the population size and the maximum number of fitness evaluations are set to 20 and 1,000 iterations, respectively. The

experiment utilizes a publicly available dataset of the coffee leaf disease dataset (<https://www.kaggle.com/datasets/auravduttaikit/coffee-leaf-diseases>), which contains 4,188 high-quality annotated images, covering four key categories: Miner with 460, No disease with 400, Phoma with 484, and Rust with 320. The experimental dataset is randomly divided into a training set (60%), a validation set (20%), and a test set

Fig. 26 An overview of the coffee leaf disease dataset

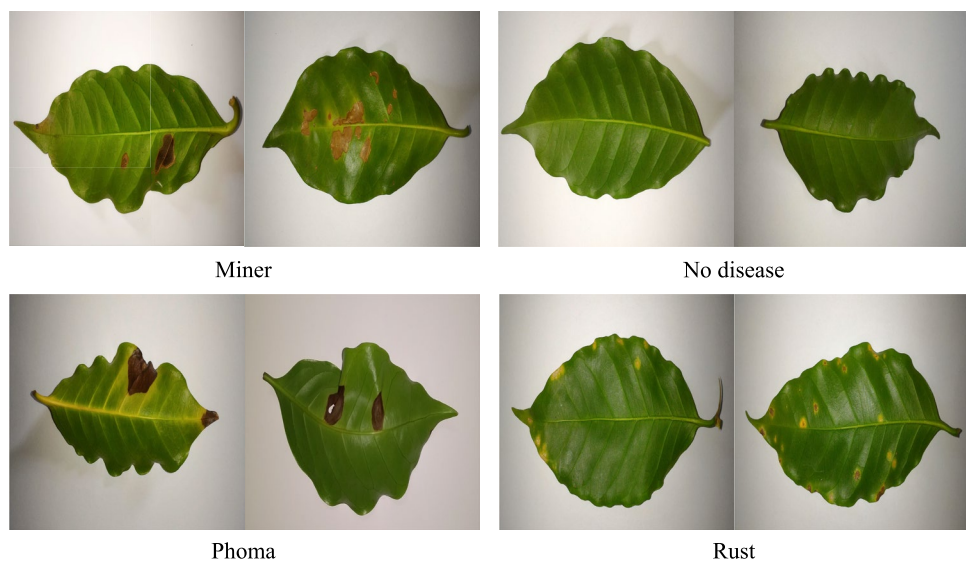


Table 10 Comparison of Experimental Outcomes

Models	Precision (%)	Accuracy (%)	Recall (%)	F1 score (%)
AlexNet	93.249 ± 0.005	93.093 ± 0.005	93.093 ± 0.005	93.079 ± 0.005
ResNet-18	94.102 ± 0.014	93.844 ± 0.016	93.844 ± 0.016	93.811 ± 0.016
VGG-16	94.746 ± 0.002	94.670 ± 0.002	94.670 ± 0.002	94.665 ± 0.002
Inception	93.412 ± 0.010	93.243 ± 0.011	93.243 ± 0.011	93.211 ± 0.011
MobileNet-v2	97.063 ± 0.003	96.997 ± 0.004	96.997 ± 0.004	96.999 ± 0.004
Swin Transformer	98.368 ± 0.003	98.348 ± 0.003	98.348 ± 0.003	98.347 ± 0.003
ConvNeXt	96.941 ± 0.002	96.922 ± 0.002	96.922 ± 0.002	96.901 ± 0.003
ASHADE-MPC-Ensemble	99.306 ± 0.001	99.300 ± 0.001	99.300 ± 0.001	99.299 ± 0.001

(20%). This proportion ensures that the model learns features sufficiently and can effectively evaluate its generalization ability. Figure 26 visually presents the composition of the dataset and the visual differences between categories. The experimental design provides a rigorous validation framework to verify the effectiveness of the ASHADE-MPC-Ensemble model in the coffee leaf disease identification.

To conduct a comprehensive performance analysis, this study selects eight representative deep learning models as evaluation benchmarks: AlexNet [51], ResNet-18 [52], VGG-16 [53], Inception [54], MobileNet-v2 [55], Swin Transformer [56], and ConvNeXt [57]. These models encompass a wide spectrum of architectural paradigms, ranging from conventional convolutional neural networks (CNNs) to modern Transformer-based frameworks, thereby providing multidimensional perspectives for comparative analysis.

The experimental configuration ensures methodological consistency through unified implementation using the PyTorch

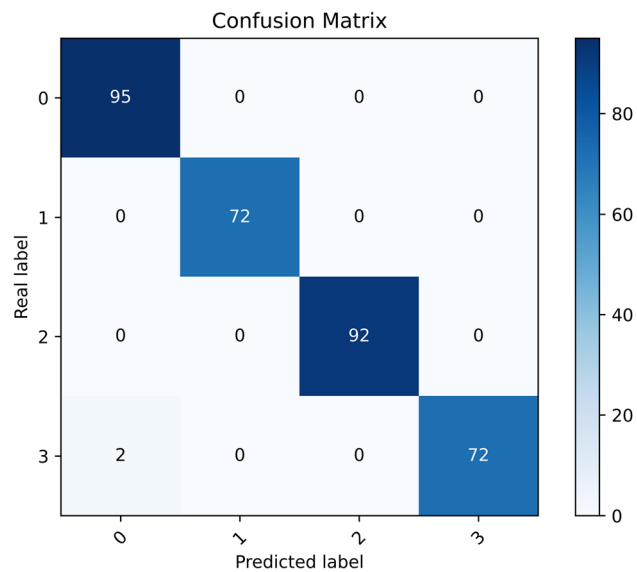


Fig. 27 Confusion matrix of the optimal ASHADE-MPC-Ensemble model where accuracy is 99.399%, precision is 99.412%, recall is 99.398%, and F1 score is 99.399%

library [58]. To mitigate the impact of randomness on experimental outcomes, each model undergoes 30 independent training-evaluation cycles, with final results derived from statistical averaging to enhance conclusion reliability and robustness. This systematic approach establishes a rigorous evaluation framework, offering both theoretical and empirical foundations for subsequent research and practical applications.

6.3 Experimental results and analysis

Table 10 summarizes the experimental outcomes of ASHADE-MPC-Ensemble when pitted against deep learning models for coffee leaf disease detection. Meanwhile,

Fig. 27 shows the confusion matrix of the optimal ASHADE-MPC-Ensemble model.

The proposed ASHADE-MPC-Ensemble model demonstrates significant performance enhancements, which achieves improvements of 0.952% in accuracy, 0.938% in precision, 0.952% in recall, and 0.952% in F1-score compared to the second-best model, Swin Transformer. These results underscore the effectiveness of the ASHADE-MPC-Ensemble framework in integrating the complementary strengths of multiple pre-trained deep learning models while optimizing the weights through an efficient ASHADE-MPC algorithm.

The observed performance highlights the robustness and adaptability of the ASHADE-MPC-Ensemble in tackling complex coffee leaf disease detection, which often involves subtle variations in visual patterns across classes. Such improvements reflect the superior predictive capability and potential scalability of ASHADE-MPC-Ensemble to other real-world scenarios, which is a state-of-the-art approach in the domain of ensemble learning and disease detection.

7 Conclusion

To address complex optimization challenges, this study proposes ASHADE-MPC, an innovative methodology comprising two core components that enhance performance: (i) a multi-agent participated competition mechanism, and (ii) an adaptive mutation probability. The competitive framework introduces two novel mutation strategies - DE/cur-to-mean($\mathbf{x}_{idx1}^t, \mathbf{x}_{idx2}^t$)/1 and DE/cur-to-mean($\mathbf{x}_{best}^t, \mathbf{x}_{idx}^t$)/1 - designed to prevent premature convergence to local optima while enhancing population diversity. The adaptive probability mechanism enables intelligent switching between global exploration and local exploitation, dynamically balancing these crucial optimization aspects throughout the search process. With rigorous statistical analysis as support, comprehensive validation is carried out via numerical experiments on CEC2017, 2020, and 2022 benchmarks, along with seven real-world engineering problems. The results show that ASHADE-MPC outperforms twelve cutting-edge optimization algorithms. Furthermore, we develop ASHADE-MPC-Ensemble by applying transfer learning to eight pretrained deep models on a coffee leaf disease dataset. The top three performing models are integrated through a soft voting framework optimized by ASHADE-MPC, with experimental results confirming the ensemble's efficacy.

However, the proposed ASHADE-MPC method still has several limitations. First, the initial values of the scaling factor (F) and crossover probability (Cr) in the algorithm still rely on manual setting, making its performance sensitive to parameter initialization. This may affect the stability and convergence behavior of the optimization process. Second,

the potential of the Multi-agent Participated Competition Mechanism (MPC) as an independent and general-purpose optimization module has not been fully explored. Specifically, the study did not conduct experiments to isolate the MPC mechanism from the SHADE framework and transplant it into other types of metaheuristic algorithms, in order to examine whether it can similarly enhance optimization performance across different algorithmic frameworks. In addition, the ASHADE-MPC integrated diagnostic model developed in this study is based on a specific coffee leaf disease dataset, and its generalization ability to other crop disease datasets or broader agricultural disease identification tasks remains to be further validated and investigated.

Although ASHADE-MPC demonstrates competitive performance in addressing complex optimization problems and agricultural disease diagnosis tasks, several promising directions remain for future work. First, to enhance algorithm robustness and reduce sensitivity to manual parameter tuning, automated strategies such as adaptive mechanisms or Bayesian optimization could be investigated to intelligently initialize and adjust the scaling factor (F) and crossover probability (Cr). Second, the generalizability of the Multi-agent Participated Competition Mechanism (MPC) as an independent and universal optimization module warrants further exploration. Specifically, future studies should focus on isolating MPC from the SHADE framework and transplanting it into other metaheuristic algorithms (e.g., Particle Swarm Optimization, Grey Wolf Optimizer,) to validate its cross-algorithm effectiveness and promote its potential as a plug-and-play optimization component. Third, the agricultural diagnostic model developed in this study is currently based on a single coffee leaf disease dataset; extending its evaluation to more diverse crop diseases and heterogeneous datasets will be essential to verify its generalization capability in real-world precision agriculture applications. Moreover, the scalability of ASHADE-MPC to high-dimensional and large-scale optimization problems, such as neural architecture search and engineering design, remains to be investigated, along with its integration into hybrid or multi-objective optimization frameworks. These future efforts aim to broaden the theoretical foundation, practical utility, and adaptability of the proposed approach across diverse complex problem domains.

Appendix: Mathematical models of engineering problems

A1 Mathematical model of Cantilever Beam Design Problem (CBDP)

The mathematical model of the Cantilever Beam Design Problem (CBDP) is formulated in Eq. (17).

$$\begin{aligned} \min f(X) &= 0.0624(x_1 + x_2 + x_3 + x_4 + x_5) \\ \text{s.t. } g(X) &= \frac{61}{x_1^3} + \frac{37}{x_2^3} + \frac{19}{x_3^3} + \frac{7}{x_4^3} + \frac{1}{x_5^3} - 1 \leq 0 \quad (17) \\ \text{where } 0.01 &\leq x_i \leq 100, i \in \{1, 2, 3, 4, 5\} \end{aligned}$$

A2 Mathematical model of Corrugated Bulkhead Design Problem (CBHDP)

The mathematical model of the Corrugated Bulkhead Design Problem (CBHDP) is formulated in Eq. (18).

$$\begin{aligned} \min f(X) &= \frac{5.885x_4(x_1 + x_3)}{x_1 + \sqrt{|x_3^2 - x_2^2|}} \\ \text{s.t. } g_1(X) &= -x_4x_2(0.4x_1 + \frac{x_3}{6}) + 8.94(x_1 + \sqrt{|x_3^2 - x_2^2|}) \leq 0 \\ g_2(X) &= -x_4x_2^2(0.2x_1 + \frac{x_3}{12}) + 2.2(8.94(x_1 + \sqrt{|x_3^2 - x_2^2|}))^{4/3} \leq 0 \\ g_3(X) &= -x_4 + 0.0156x_1 + 0.15 \leq 0 \\ g_4(X) &= -x_4 + 0.0156x_3 + 0.15 \leq 0 \\ g_5(X) &= -x_4 + 1.05 \leq 0 \\ g_6(X) &= -x_3 + x_2 \leq 0 \\ \text{where } 0 \leq &x_1, x_2, x_3 \leq 100 \\ 0 \leq &x_4 \leq 5 \end{aligned} \quad (18)$$

A3 Mathematical model of Gear Train Design Problem (GTDP)

The mathematical model of the Gear Train Design Problem (GTDP) is formulated in Eq. (19).

$$\begin{aligned} \min f(X) &= \left(\frac{1}{6.931} - \frac{x_3x_2}{x_1x_4} \right)^2 \\ \text{where } x_1, x_2, x_3, x_4 &\in \{12, 13, 14, \dots, 60\} \end{aligned} \quad (19)$$

A4 Mathematical model of Speed Reducer Design Problem (SRDP)

The mathematical model of the Speed Reducer Design Problem (SRDP) is formulated in Eq. (20).

$$\begin{aligned} \min f(X) &= 0.7854x_1x_2^2(3.3333x_3^2 + 14.9334x_3 - 43.0924) - 1.508x_1(x_6^2 + x_7^2) \\ &\quad + 7.4777(x_6^3 + x_7^3) + 0.7854(x_4x_6^2 + x_5x_7^2) \\ \text{s.t. } g_1(X) &= \frac{27}{x_1x_2^2x_3} - 1 \leq 0 \\ g_2(X) &= \frac{397.5}{x_1x_2^2x_3^2} - 1 \leq 0 \\ g_3(X) &= \frac{1.93x_4^3}{x_2x_6^4x_3} - 1 \leq 0 \\ g_4(X) &= \frac{1.93x_5^3}{x_2x_7^4x_3} - 1 \leq 0 \\ g_5(X) &= \frac{\sqrt{(745x_4/x_2x_3)^2 + 16900000}}{110x_6^3} - 1 \leq 0 \\ g_6(X) &= \frac{\sqrt{(745x_5/x_2x_3)^2 + 157500000}}{85x_7^3} - 1 \leq 0 \\ g_7(X) &= \frac{x_2x_3}{40} - 1 \leq 0 \\ g_8(X) &= \frac{5x_2}{x_1} - 1 \leq 0 \\ g_9(X) &= \frac{x_1}{12x_2} - 1 \leq 0 \\ g_{10}(X) &= \frac{1.5x_6 + 1.9}{x_4} - 1 \leq 0 \\ g_{11}(X) &= \frac{1.1x_7 + 1.9}{x_5} - 1 \leq 0 \\ \text{where } 2.6 \leq &x_1 \leq 2.6 \\ 0.7 \leq &x_2 \leq 0.8 \\ 17 \leq &x_3 \leq 28 \\ 7.3 \leq &x_4x_5 \leq 8.3 \\ 2.9 \leq &x_6 \leq 3.9 \\ 5 \leq &x_7 \leq 5.5 \end{aligned} \quad (20)$$

A5 Mathematical model of Three Bar Truss Design Problem (TBTDP)

The mathematical model of the Three Bar Truss Design Problem (TBTDP) is formulated in Eq. (21).

$$\begin{aligned} \min f(X) &= (2\sqrt{2}x_1 + x_2) \cdot l \\ \text{s.t. } g_1(X) &= \frac{\sqrt{2}x_1 + x_2}{\sqrt{2}x_1^2 + 2x_1x_2} P - \sigma \leq 0 \\ g_2(X) &= \frac{x_2}{\sqrt{2}x_1^2 + 2x_1x_2} P - \sigma \leq 0 \\ g_3(X) &= \frac{1}{\sqrt{2}x_2 + x_1} P - \sigma \leq 0 \end{aligned} \quad (21)$$

$$l = 100 \text{ cm}, P = 2kN/cm^3, \sigma = 2kN/cm^3$$

where $0 \leq x_1, x_2 \leq 1$

A6 Mathematical model of Tubular Column Design Problem (TCDP)

The mathematical model of the Three Bar Truss Design Problem (TBTDP) is formulated in Eq. (22).

$$\begin{aligned} \min f(X) &= 9.8x_1x_2 + 2x_1 \\ \text{s.t. } g_1(X) &= \frac{P}{\pi x_1 x_2 \sigma_y} - 1 \leq 0 \\ g_2(X) &= \frac{8PL^2}{\pi^3 E x_1 x_2 (x_1^2 + x_2^2)} - 1 \leq 0 \end{aligned} \quad (22)$$

where $2 \leq x_1 \leq 14$

$0.2 \leq x_2 \leq 0.8$

A7 Mathematical model of Welded Beam Design Problem (WBDP)

The mathematical model of the Three Bar Truss Design Problem (TBTDP) is formulated in Eq. (23).

$$\begin{aligned} \min f(X) &= 1.10471x_1^2x_2 + 0.04811x_3x_4(14 + x_2) \\ \text{s.t. } g_1(X) &= \tau(X) - \tau_{max} \leq 0 \\ g_2(X) &= \sigma(X) - \sigma_{max} \leq 0 \\ g_3(X) &= \delta(X) - \delta_{max} \leq 0 \\ g_4(X) &= x_1 - x_4 \leq 0 \\ g_5(X) &= P - P_c(X) \leq 0 \\ g_6(X) &= 0.125 - x_1 \leq 0 \\ g_7(X) &= 1.10471x_1^2x_2 + 0.04811x_3x_4(14 + x_2) - 5 \leq 0 \end{aligned} \quad (23)$$

where $0.1 \leq x_1, x_4 \leq 2$
 $0.1 \leq x_2, x_3 \leq 10$

B Detailed results of comparison experiments in CEC2017

Tables 11, 12, 13, and 14 summarize the detailed experimental results and statistical analysis in CEC2017 benchmark functions.

Table 11 Results of comparison experiments in 30-D CEC2017

Func.	DE	PSO	CMA-ES	L-SHADE	jSO	L-SHADE- cnEpsSin	CSO	MCSO	L-SHACSO	CDE	CDEKI	ISHACDE	ASHADE-MPC
f_1	mean	2.336e+10	6.034e+09	2.352e+09	2.182e+03	8.255e+07	2.525e+08 +	2.414e+03	1.325e+05	2.432e+03	1.981e+03	9.405e+02	1.018e+02
	std	4.369e+09	2.006e+09	1.907e-06	0.000e+00	1.005e+08	2.014e+08	+ +	+ +	+ +	+ +	+ +	
f_3	mean	2.380e+05	1.154e+05	1.418e+04	8.183e+04	2.199e+04	3.527e+04 \approx	5.194e+04	2.364e+04	1.549e+03	2.523e+03	2.805e+03	4.429e+03
	std	3.675e+04	2.198e+04	1.091e-11	4.366e-11	4.172e+03	6.836e+03	+ +	+ +	3.187e+04	5.795e+04	4.207e+04	5.978e+04
f_4	mean	1.957e+03	2.783e+03	5.237e+02	5.119e+02	6.306e+02	5.824e+02 +	5.111e+02	5.140e+02	5.140e+02	4.293e+02	4.540e+02	4.759e+02
	std	4.728e+02	1.896e+03	2.274e-13	2.842e-13	8.347e+01	4.972e+01	+ +	+ +	+ +	+ +	- -	$\approx \approx$
f_5	mean	8.402e+02	8.395e+02	7.150e+02	6.313e+02	7.994e+02	8.016e+02 +	5.189e+02	6.650e+02	5.125e+02 -	6.716e+02	5.951e+02	6.109e+02
	std	2.388e+01	4.976e+01	1.137e-13	5.684e-13	6.484e+00	3.578e+00	4.568e+00	9.360e+00	3.729e+00	2.196e+01	4.915e+01	2.482e+01
f_6	mean	6.594e+02	6.638e+02	6.260e+02	6.007e+02	6.652e+02	6.654e+02	6.000e+02	6.003e+02	6.000e+02	6.002e+02	6.019e+02	6.000e+02
	std	6.936e+00	1.253e+01	5.684e-13	2.274e-13	1.016e+00	9.627e-01	+ +	+ +	+ +	+ +	+ +	
f_7	mean	1.860e+03	1.216e+03	1.059e+03	8.583e+02	1.306e+03	1.312e+03 +	7.430e+02	9.035e+02	7.491e+02 -	9.188e+02	8.992e+02	8.577e+02
	std	1.863e+02	9.326e+01	4.547e-13	6.821e-13	1.195e+01	7.279e+00	- -	- -	- -	- -	- -	$\approx \approx$
f_8	mean	1.155e+03	1.115e+03	1.026e+03	9.101e+02	9.951e+02	9.980e+02 +	- -	- -	- -	- -	- -	9.637e-02
	std	1.934e+01	4.188e+01	6.821e-13	1.137e-13	4.387e+00	3.661e+00	4.599e+00	1.153e+01	3.015e+00	2.657e+01	7.003e+01	2.792e+01
f_9	mean	1.392e+04	1.043e+04	3.399e+03	9.218e+02	6.240e+03	7.261e+03 +	- -	- -	8.122e+02 -	9.610e+02	8.954e+02	9.177e+02
	std	1.651e+03	2.942e+03	1.819e-12	7.958e-13	6.909e+02	3.129e+02	5.077e-01	7.892e-02	1.253e+02	3.204e+01	5.608e+01	1.857e+01
f_{10}	mean	7.795e+03	8.767e+03	9.179e+03	6.670e+03	5.256e+03	5.356e+03 -	- -	- -	2.609e+03 -	8.231e+03	8.410e+03	6.398e+03
	std	5.359e+02	2.913e+02	3.638e-12	5.457e-12	1.799e+02	1.468e+02	5.208e+02	4.042e+02	4.399e+02	3.430e+02	3.688e+02	4.700e+02
f_{11}	mean	2.054e+03	5.574e+03	1.314e+03	1.267e+03	1.214e+03	1.277e+03 +	+ +	+ +	$\approx \approx$	+ +	+ +	$\approx \approx$
	std	2.013e+02	2.645e+03	4.547e-13	1.137e-12	3.363e+01	4.666e+01	6.386e+01	2.268e+01	3.467e+01	3.794e+01	2.676e+01	1.108e+02
f_{12}	mean	7.205e+08	8.711e+08	1.995e+05	7.373e+05	1.168e+06	5.138e+06 +	1.106e+06	7.748e+05	7.053e+05	1.784e+05	4.258e+04	3.366e+04
	std	1.912e+08	7.997e+08	8.731e-11	0.000e+00	1.234e+06	4.841e+06	+ +	+ +	+ +	+ +	+ +	$\approx \approx$
f_{13}	mean	1.266e+07	1.808e+07	2.435e+03	6.069e+04	1.649e+04	3.727e+04 +	1.130e+04	1.193e+04	1.090e+04	1.398e+04	1.237e+04	1.959e+04
	std	6.509e+06	6.291e+08	1.819e-12	3.638e-11	5.374e+03	1.232e+04	6.173e+03	6.096e+03	4.221e+03	9.359e+03	1.240e+04	5.690e+04
f_{14}	mean	1.700e+03	9.923e+05	1.482e+03	1.558e+03	1.522e+03	2.467e+03 +	+ +	+ +	1.255e+05	3.140e+03	8.233e+03	1.532e+04
	std	3.486e+01	1.133e+06	0.000e+00	2.274e-13	3.795e+01	2.972e+03	2.072e+05	6.210e+04	5.247e+04	1.814e+03	5.236e+03	5.246e+04

Table 11 (continued)

Func.	DE	PSO	CMA-ES	L-SHADE	jSO	L-SHADE- cnEpsin	CSO	MCSO	L-SHACSO	CDE	CDEKI	ISHACDF	ASHADE-MPC
f_{15}	mean	1.474e+04	4.015e+05	1.616e+03	4.874e+03	1.896e+03	3.777e+03	+	2.832e+03	2.709e+03	2.107e+03	5.213e+03	1.083e+04 1.607e+03 2.028e+03
	std	4.561e+03	1.575e+06	0.000e+00	3.638e-12	1.895e+02	7.861e+02	-	+ +	+ +	+ +	-	-
f_{16}	mean	3.568e+03	4.172e+03	3.559e+03	2.599e+03	3.028e+03	3.119e+03	+	1.407e+03	1.382e+03	5.284e+02	3.317e+03	1.043e+04 7.991e+01 2.539e+03
	std	3.453e+02	2.556e+02	4.547e-13	2.274e-12	2.908e+02	2.289e+02	-	-	-	-	-	-

Table 12 Results of comparison experiments in 30-D CEC2017 (Continued)

Func.	DE	PSO	CMA-ES	L-SHADE	jSO	L-SHADE-cnEpsin	CSO	MCSO	L-SHACSO	CDE	CDEKI	ISHACDDE	ASHADE-MPC
f_{17} mean	2.425e+03	3.013e+03	2.504e+03	2.035e+03	2.046e+03	2.670e+03	2.670e+03 +	1.837e+03	1.824e+03	1.810e+03	1.963e+03	1.892e+03	2.028e+03
std	+ +	+ +	+ +	+ +	+ +	+ +	- -	- -	- -	+ +	~ ~	+ +	1.905e+03
f_{18} mean	1.844e+02	2.158e+02	1.364e+12	2.501e+12	2.276e+02	2.061e+02	1.141e+02	7.044e+01	9.943e+01	1.044e+02	1.331e+02	1.066e+02	6.925e+01
std	1.737e+06	1.532e+07	1.874e+03	3.374e+05	2.437e+04	6.606e+04 +	4.827e+05	6.010e+05	3.223e+05	4.255e+05	3.859e+05	3.050e+05	2.937e+04
f_{19} mean	8.914e+05	4.966e+05	1.928e+03	5.649e+03	3.316e+03	4.194e+03 +	4.359e+05	4.734e+05	2.051e+05	2.745e+05	2.568e+05	6.717e+05	1.721e+04
std	+ +	- -	+ +	+ +	+ +	+ +	4.546e+03	4.747e+03	4.999e+03	6.233e+03	1.335e+04	1.234e+04	1.963e+03
f_{20} mean	5.616e+05	7.361e+05	2.046e+12	3.638e+12	1.344e+03	1.340e+03	2.177e+03	1.834e+03	1.149e+03	4.678e+03	1.360e+04	2.780e+04	2.918e+01
std	2.653e+03	3.001e+03	3.049e+03	2.434e+03	3.133e+03	3.121e+03 +	2.198e+03	2.200e+03	2.157e+03	2.460e+03	2.300e+03	2.467e+03	2.332e+03
f_{21} mean	1.766e+02	1.024e+02	9.095e-13	3.183e-12	5.300e+01	4.251e+01	6.256e+01	6.121e+01	2.553e+01	1.074e+02	1.774e+02	9.797e+01	8.665e+01
std	2.632e+03	2.631e+03	2.520e+03	2.424e+03	2.658e+03	2.661e+03 +	2.321e+03	2.456e+03	2.312e+03	2.450e+03	2.384e+03	2.410e+03	2.378e+03
f_{22} mean	1.469e+01	4.741e+01	1.364e+12	0.000e+00	7.490e+01	2.962e+01	- -	- -	- -	+ +	~ ~	+ +	+ +
std	9.639e+03	4.214e+03	2.911e+03	2.301e+03	7.681e+03	7.884e+03 +	2.300e+03	2.303e+03	2.300e+03	2.302e+03	3.799e+03	2.300e+03	2.300e+03
f_{23} mean	8.382e+02	1.484e+03	4.547e+13	2.274e+12	2.913e+02	2.655e+02	6.473e-06	4.405e-01	8.700e-03	2.516e+00	3.003e+03	1.041e+00	7.364e+01
std	2.957e+03	3.114e+03	2.947e+03	2.783e+03	4.516e+03	4.537e+03 +	- -	- -	2.661e+03	2.741e+03	2.727e+03	2.757e+03	2.716e+03
f_{24} mean	1.736e+01	6.518e+01	9.095e-13	1.819e-12	1.737e+02	1.720e+02	1.004e+01	2.607e+01	7.303e+00	3.947e+01	2.301e+01	2.696e+01	2.929e+01
std	3.097e+03	3.319e+03	3.084e+03	2.955e+03	3.106e+03	3.103e+03 +	2.843e+03	2.950e+03	2.825e+03	2.930e+03	2.904e+03	2.894e+03	2.871e+03
f_{25} mean	1.479e+01	1.088e+02	3.638e+12	1.819e-12	2.306e+02	1.032e+02	7.977e+00	3.095e+01	3.707e+00	4.581e+01	2.466e+01	3.685e+01	2.232e+01
std	4.677e+03	3.260e+03	3.316e+03	2.888e+03	2.990e+03	2.986e+03 +	- -	- -	- -	+ +	~ ~	+ +	+ +
f_{26} mean	4.419e+02	1.366e+02	2.728e+12	9.095e-13	2.296e+01	2.453e+01	9.321e+00	9.095e-01	8.639e-01	1.787e+01	1.103e+01	5.394e+00	1.020e+01
std	6.981e+03	7.824e+03	5.905e+03	5.116e+03	6.928e+03	5.890e+03 +	3.742e+03	4.346e+03	3.505e+03	4.164e+03	4.464e+03	4.482e+03	4.057e+03
f_{27} mean	1.455e+02	8.197e+02	0.000e+00	9.095e-13	1.466e+03	1.580e+03	5.033e+02	3.556e+02	4.595e+02	7.811e+02	6.726e+02	5.792e+02	4.523e+02
std	3.252e+03	3.655e+03	3.203e+03	3.221e+03	6.655e+03	6.705e+03 +	3.229e+03	3.213e+03	3.220e+03	3.241e+03	3.243e+03	3.220e+03	3.217e+03
f_{28} mean	+ +	- -	+ +	+ +	+ +	+ +	- -	- -	- -	+ +	~ ~	+ +	+ +
std	9.638e+02	7.457e+02	2.274e+12	3.183e-12	3.757e+01	6.191e+01	2.009e+01	1.521e+01	1.590e+01	2.240e+01	6.191e+01	3.168e+01	2.648e+01
f_{29} mean	4.097e+03	5.316e+03	4.123e+03	3.691e+03	3.712e+03	3.4313e+03 +	3.518e+03	3.519e+03	3.382e+03	3.807e+03	3.563e+03	3.600e+03	3.623e+03
std	3.032e+02	3.739e+02	9.095e-13	0.000e+00	1.144e+02	1.119e+02	1.015e+01	6.393e+00	5.302e+00	1.643e+01	2.245e+01	1.051e+01	1.025e+01
f_{30} mean	1.732e+01	9.876e+01	0.000e+00	1.144e+02	1.119e+02	1.069e+05 +	1.048e+04	1.381e+04	7.779e-03	1.327e+04	9.825e+03	1.378e+04	9.910e+03
std	6.326e+05	4.903e+07	7.276e+12	0.000e+00	1.524e+04	4.937e+04	3.856e+03	3.711e+03	9.599e+02	5.324e+03	3.281e+03	3.824e+04	3.977e+03

Table 12 (continued)

Func.	DE	PSO	CMA-ES	L-SHADE	jSO	L-SHADE-cnfPSSin	CSO	MCSO	L-SHACSO	CDE	CDEKI	ISHACDFE	ASHADE-MPC
+/-/≈/-:	29/0/0	29/0/0	21/2/6	24/3/2	28/1/0	27/1/1	14/1/14	22/1/6	13/2/14	27/2/0	15/9/5	20/8/1	-
Avg. rank:	11.4	12.0	7.5	6.8	8.6	9.9	4.4	6.2	3.2	6.9	5.7	5.2	3.2

Table 13 Results of comparison experiments in 50-D CEC2017

Func.	DE	PSO	CMA-ES	L-SHADE	jSO	L-SHADE-cnEpSin	CSO	MCSO	L-SHACSO	CDE	CDEKU	ISHACDE	ASHADE-MPC	
f_1	mean	5.870e+10	2.782e+10	4.183e+10	6.724e+03	3.042e+08	1.497e+09	+	1.735e+03	1.556e+04	1.619e+03 ≈	3.173e+03	5.999e+03	
	+	+	+	+	+	+	≈	+	+	≈	≈	+	1.896e+03	
std	1.044e+10	5.103e+09	1.526e-05	9.095e-12	1.939e+08	3.945e+08	1.995e+03	3.455e+03	1.727e+03	5.870e+03	8.554e+03	1.973e+03	2.529e+03	
f_3	mean	4.695e+05	2.461e+05	6.742e+04	6.634e+04	1.011e+05	≈	1.333e+05	1.148e+05	8.005e+04	1.387e+05	1.186e+05	1.421e+05	1.006e+05
	+	+	-	-	-	-	+	+	+	+	+	+	+	
std	3.781e+04	2.933e+04	4.366e-11	2.910e-11	9.128e+03	1.248e+04	1.917e+04	1.664e+04	1.380e+04	1.796e+04	1.950e+04	6.055e+04	4.198e+04	
f_4	mean	6.897e+03	6.973e+03	5.438e+03	4.713e+02	7.281e+02	8.655e+02	+	6.119e+02	5.740e+02	5.709e+02	5.737e+02	4.941e+02	5.161e+02
	+	+	+	-	+	+	+	+	+	+	-	≈	≈	
std	1.446e+03	4.713e+03	1.819e-12	3.411e-13	7.134e+01	1.191e+02	3.983e+01	3.776e+01	3.573e+01	4.167e+01	4.627e+01	5.171e+01	4.425e+01	
f_5	mean	1.170e+03	1.083e+03	1.034e+03	7.962e+02	8.747e+02	8.839e+02	+	5.476e+02	8.229e+02	5.236e+02 -	7.797e+02	6.624e+02	7.055e+02
	+	+	+	+	+	+	+	+	+	+	-	+	6.764e+02	
std	2.570e+01	1.029e+02	6.821e-13	2.274e-13	1.042e+01	5.461e+00	8.436e+00	1.586e+01	4.860e+00	1.009e+02	6.210e+01	4.614e+01	4.524e+01	
f_6	mean	6.676e+02	6.861e+02	6.506e+02	6.001e+02	6.692e+02	6.697e+02	+	6.000e+02	6.000e+02	6.000e+02 ≈	6.029e+02	6.086e+02	6.002e+02
	+	+	+	+	+	+	≈	+	+	+	+	+	+	
std	7.539e+00	1.216e+01	6.821e-13	4.547e-13	9.903e-01	5.189e-01	2.887e-02	1.398e-02	6.790e-04	1.978e+00	4.157e+00	5.752e-01	1.215e-02	
f_7	mean	3.099e+03	1.707e+03	1.614e+03	1.022e+03	1.769e+03	+	7.792e+02	1.087e+03	7.697e+02 -	1.157e+03	1.056e+03	9.824e+02	9.499e+02
	+	+	+	+	+	+	+	+	+	+	+	+	+	
std	3.053e+02	1.402e+02	0.000e+00	1.137e-12	1.139e+01	5.016e+00	6.551e+00	1.293e+01	5.809e+00	4.376e+01	1.238e+01	5.747e+01	4.247e+01	
f_8	mean	1.451e+03	1.410e+03	1.328e+03	1.076e+03	1.216e+03	1.221e+03	+	8.500e+02	1.124e+03	8.242e+02 -	1.075e+03	9.727e+02	1.016e+03
	+	+	+	+	+	+	+	+	+	+	+	+	+	
std	4.903e+01	1.120e+02	1.364e-12	6.821e-13	1.019e+01	4.267e+00	7.071e+00	1.581e+01	4.730e+00	9.615e+01	7.943e+01	5.342e+01	4.031e+01	
f_9	mean	3.833e+04	3.331e+04	9.113e+04	9.113e+02	1.627e+04	2.1595e+04	+	9.266e+02	9.001e+02	9.001e+02 -	2.858e+03	6.891e+03	1.037e+03
	+	+	+	+	-	+	≈	-	-	+	+	+	+	
std	6.169e+03	7.397e+03	1.273e+11	1.137e-13	1.969e+03	1.2745e+03	2.785e+01	1.063e-01	1.962e-01	1.381e+03	3.151e+03	1.580e+02	6.297e+01	
f_{10}	mean	1.398e+04	1.521e+04	1.527e+04	1.029e+04	8.025e+03	1.2575e+04	+	4.249e+03	1.241e+04	3.286e+03 -	1.436e+04	1.449e+04	1.041e+04
	+	+	+	-	-	-	+	+	+	+	+	+	-	
std	1.245e+03	3.116e+02	1.091e-11	1.273e-11	3.198e+02	3.361e+02	6.030e+02	5.545e+02	5.768e+02	3.510e+02	5.148e+02	5.705e+02	1.224e+03	
f_{11}	mean	8.634e+03	1.594e+04	1.572e+03	1.575e+03	1.399e+03	1.805e+03	1.991e+03	1.680e+03	1.875e+03	1.255e+03	1.210e+03	1.657e+03	1.224e+03
	+	+	+	+	+	+	+	+	+	+	-	+	+	
std	2.213e+03	6.354e+03	1.137e-12	4.547e-13	7.855e+01	1.153e+02	6.753e+02	2.474e+02	3.281e+02	3.382e+01	3.435e+01	9.598e+02	3.529e+01	
f_{12}	mean	6.252e+09	3.732e+09	3.3872e+08	3.3872e+06	6.109e+06	1.1025e+08	+	3.523e+06	2.516e+06	2.243e+06	1.5995e+06	4.295e+05	2.391e+05
	+	+	+	+	+	+	+	+	+	+	+	+	-	
std	1.678e+09	4.553e+09	1.192e+07	0.000e+00	3.279e+06	5.953e+07	1.744e+06	8.709e+05	5.926e+05	1.022e+06	2.503e+05	3.188e+05	2.208e+05	
f_{13}	mean	5.024e+08	7.264e+08	3.879e+04	2.615e+04	1.673e+04	6.9525e+04	+	4.491e+03	2.362e+03	2.114e+03 -	4.889e+03	6.964e+03	3.791e+03
	+	+	+	+	+	+	≈	-	-	+	+	+	-	
std	2.128e+08	1.115e+09	1.455e-11	1.455e-11	5.965e+03	5.479e+04	2.903e+03	1.239e+03	5.162e+02	3.189e+03	5.628e+03	2.364e+03	2.911e+03	
f_{14}	mean	2.205e+05	7.577e+06	1.574e+03	4.186e+03	3.497e+03	1.209e+04	7.144e+05	1.903e+05	3.141e+05	7.290e+04	4.967e+04	5.121e+03	
	+	+	-	≈	-	-	+	+	+	+	+	+	+	
std	2.657e+05	6.299e+06	2.274e+12	2.728e+12	2.685e+03	6.663e+03	4.801e+05	1.385e+05	1.646e+05	5.095e+04	5.111e+04	2.505e+05	5.114e+03	
f_{15}	mean	6.819e+07	1.309e+07	2.307e+13 ≈	1.338e+04	1.233e+04	1.6305e+04	5.903e-03	5.145e+03	6.001e+03	8.119e+03	5.924e+03	3.066e+03	
	+	+	+	+	+	+	+	+	+	+	+	+	+	
std	2.089e+08	1.814e+07	2.274e+12	3.638e+12	4.097e+03	2.8625e+03	3.114e+03	2.164e+03	1.838e+03	4.687e+03	5.062e+03	3.616e+03	1.569e+03	

Table 13 (continued)

Func.	DE	PSO	CMA-ES	L-SHADE	jSO	L-SHADE-cnEpSin	CSO	MCSO	L-SHACSO	CDE	CDEKI	ISHACDE	ASHADE-MPC
f_{16}^{mean}	5.950e+03	6.375e+03	5.046e+03	3.089e+03	3.105e+03	3.827e+03 +	2.445e+03	2.179e+03	2.087e+03 -	3.837e+03	3.071e+03	3.278e+03	2.980e+03
+	+	+	+	+	+	-	-	-	+	~	~	+	+
std	3.206e+02	6.714e+02	3.638e-12	0.000e+00	1.976e+02	2.289e+02	3.370e+02	2.683e+02	1.386e+02	5.610e+02	9.225e+02	5.671e+02	2.816e+02

Table 14 Results of comparison experiments in 50-D CEC2017 (Continued)

Func.	DE	PSO	CMA-ES	L-SHADE	jSO	L-SHADEnEpSin	CSO	MCSO	L-SHACSO	CDE	CDEKI	ISHACDE	ASHADE-MPC
f_{17} mean	4.705e+03	4.876e+03	4.005e+03	3.215e+03	2.871e+03	3.215e+03	+	2.368e+03	2.428e+03	2.114e+03 –	3.349e+03	3.036e+03	3.089e+03
f_{17} std	+	+	+	+	~	~	–	–	–	+	~	+	2.850e+03
f_{18} mean	2.777e+02	5.070e+02	5.002e+02	2.274e+12	2.432e+02	1.747e+02	2.311e+02	3.728e+02	1.964e+02	3.301e+02	5.519e+02	2.943e+02	2.258e+02
f_{18} std	8.425e+06	5.202e+07	9.506e+03	1.425e+06	1.151e+05	3.303e+05	+	2.389e+06	1.905e+06	1.730e+06	2.001e+06	9.534e+05	4.528e+05
f_{19} mean	+	+	–	+	~	~	+	+	+	+	+	+	+
f_{19} std	5.108e+06	3.643e+07	1.819e+12	9.313e+10	7.460e+04	1.894e+05	1.244e+06	7.613e+05	4.806e+05	1.060e+06	7.122e+05	1.202e+06	5.078e+04
f_{19} mean	4.968e+06	8.970e+06	2.034e+03	3.109e+04	4.569e+04	4.569e+04	1.506e+04	1.528e+04	1.564e+04	1.766e+04	1.423e+04	1.006e+04	2.100e+03
f_{20} mean	+	+	–	+	+	+	+	+	+	+	+	+	+
f_{20} std	4.348e+06	2.594e+07	0.000e+00	7.276e+12	4.226e+03	2.300e+04	5.156e+03	3.774e+03	2.579e+03	8.155e+03	1.159e+04	9.004e+03	1.751e+02
f_{20} mean	3.685e+03	4.230e+03	4.202e+03	3.335e+03	3.673e+03	3.521e+03	–	–	–	3.629e+03	3.528e+03	3.279e+03	3.094e+03
f_{21} mean	3.131e+02	1.542e+02	1.819e+12	2.274e+12	7.819e+01	1.404e+02	1.839e+02	1.515e+02	1.489e+02	1.885e+02	5.917e+02	2.054e+02	1.6333e+02
f_{21} std	2.959e+03	2.939e+03	2.794e+03	2.546e+03	2.821e+03	2.610e+03	+	2.343e+03	2.613e+03	2.322e+03	2.583e+03	2.454e+03	2.450e+03
f_{22} mean	3.264e+01	9.299e+01	9.095e+13	6.704e+01	1.583e+01	7.754e+00	1.828e+01	4.170e+00	9.094e+01	6.156e+01	6.322e+01	4.248e+01	–
f_{22} std	1.650e+04	1.672e+04	1.658e+04	6.239e+03	1.292e+04	9.420e+03	~	3.832e+03	4.738e+03	2.300e+03	1.403e+04	1.559e+04	1.160e+04
f_{23} mean	4.921e+02	5.451e+02	7.276e+12	0.000e+00	3.339e+02	3.191e+03	1.841e+03	4.578e+03	1.454e+02	4.744e+03	2.776e+03	3.199e+03	5.290e+03
f_{23} std	3.369e+03	3.732e+03	3.395e+03	3.012e+03	5.124e+03	3.133e+03	–	2.805e+03	2.917e+03	2.751e+03	2.915e+03	2.925e+03	2.883e+03
f_{24} mean	3.010e+01	1.274e+02	1.819e+12	4.547e+13	1.512e+02	3.498e+01	1.728e+01	5.422e+01	1.025e+01	8.503e+01	4.603e+01	6.323e+01	3.974e+01
f_{24} std	3.466e+03	3.911e+03	3.443e+03	3.186e+03	3.117e+03	3.246e+03	+	2.961e+03	3.016e+03	2.909e+03	3.119e+03	3.113e+03	3.038e+03
f_{25} mean	2.292e+01	9.118e+01	1.364e+12	0.000e+00	8.921e+01	5.457e+01	1.477e+01	9.078e+01	7.493e+00	8.782e+01	5.490e+01	6.797e+01	4.041e+01
f_{25} std	1.107e+04	6.195e+03	3.813e+03	3.088e+03	3.279e+03	3.462e+03	+	3.113e+03	3.065e+03	3.086e+03	3.102e+03	3.041e+03	3.050e+03
f_{26} mean	2.278e+03	8.673e+02	4.547e+12	4.547e+13	5.128e+01	3.601e+01	3.323e+01	1.622e+01	1.447e+01	2.745e+01	4.331e+01	3.461e+01	3.436e+01
f_{26} std	1.047e+04	1.349e+04	1.006e+04	6.529e+03	1.248e+04	7.918e+03	–	4.834e+03	4.319e+03	4.149e+03	5.928e+03	6.332e+03	5.415e+03
f_{27} mean	3.976e+02	1.463e+03	7.276e+12	9.095e+13	7.988e+02	3.882e+02	5.3335e+02	5.165e+02	4.760e+02	6.226e+02	8.914e+02	8.486e+02	9.389e+02
f_{27} std	3.545e+03	5.032e+03	3.364e+03	3.265e+03	1.048e+04	3.628e+03	+	3.426e+03	3.285e+03	3.320e+03	3.520e+03	3.487e+03	3.373e+03
f_{28} mean	+	+	~	–	+	+	+	–	–	+	+	~	–
f_{28} std	3.319e+02	1.122e+03	9.095e+13	2.274e+12	5.928e+01	1.507e+02	5.202e+01	2.487e+01	2.061e+01	3.878e+01	3.001e+01	2.580e+01	3.166e+01
f_{29} mean	6.343e+03	8.829e+03	5.588e+03	4.100e+03	4.134e+03	5.062e+03	+	3.771e+03	3.464e+03	3.532e+03	4.076e+03	4.015e+03	3.864e+03
f_{29} std	2.990e+02	1.945e+03	1.819e+12	1.819e+12	2.948e+02	2.118e+02	2.398e+02	1.453e+02	1.749e+02	2.903e+02	2.991e+02	2.546e+02	1.750e+02
f_{30} mean	1.353e+08	4.203e+08	2.595e+06	6.276e+06	2.384e+06	2.718e+07	1.312e+06	8.926e+05	9.348e+05	1.084e+06	1.578e+06	9.471e+05	8.747e+05
f_{30} std	6.563e+07	3.992e+08	2.328e+09	9.313e+10	5.610e+05	8.079e+06	2.529e+05	6.518e+04	6.090e+04	2.067e+05	5.113e+05	1.286e+05	1.266e+05

Table 14 (continued)

Func.	DE	PSO	CMA-ES	L-SHADE	jSO	L-SHADE-cnfPSSin	CSO	MCSO	L-SHACSO	CDE	CDEKI	ISHACDFE	ASHADE-MPC
+/ \approx /-:	29/0/0	29/0/0	21/1/7	26/1/2	25/1/3	28/1/0	11/5/13	17/3/9	10/3/16	26/3/0	19/5/5	18/7/4	-
Avg. rank:	11.9	12.4	8.7	6.0	8.2	9.3	4.8	5.0	3.2	7.2	5.7	5.1	3.5

C Detailed results of comparison experiments in CEC2020

Tables 15 and 16 summarize the detailed experimental results and statistical analysis in CEC2020 benchmark functions.

Table 15 Results of comparison experiments in 10-D CEC2020

Func.	DE	PSO	CMA-ES	L-SHADE	jSO	L-SHADEnEpSIn	CSO	MCSO	L-SHACSO	CDE	CDEKI	ISHACDIE	ASHADE-MPC		
f_1	mean	2.937e+08	4.791e+08	1.663e+05	4.580e+05	9.148e+08	1.374e+06	+	5.981e+02	2.647e+06	5.270e+02 ≈	9.303e+02	1.835e+03	8.186e+04	6.630e+02
	std	+	+	+	+	+	+	≈	+	+	≈	+	+	+	
f_2	mean	1.140e+08	6.424e+08	1.164e-10	1.746e-10	9.871e+08	2.590e+06	4.958e+02	7.668e+05	4.129e+02	1.197e+03	2.309e+03	3.572e+05	9.204e+02	
	std	1.814e+10	1.038e+10	2.859e+03	1.871e+03	2.848e+03	2.007e+06	-	1.377e+03	2.358e+03	5.539e+04	2.137e+03	2.275e+03	2.172e+03	2.064e+03
f_3	mean	+	+	+	+	+	+	-	+	+	≈	+	+	+	
	std	6.055e+09	2.168e+10	3.638e-12	2.274e-12	8.259e+01	4.290e+06	2.344e+02	1.778e+02	4.600e+04	2.155e+02	3.593e+02	1.879e+02	2.175e+02	
f_4	mean	1.102e+10	1.792e+09	8.010e+02	7.502e+02	3.932e+03	6.812e+05	+	7.402e+02	8.388e+02	4.635e+04	7.384e+02	7.434e+02	7.457e+02	7.382e+02
	std	3.376e+09	2.432e+09	2.274e-13	0.000e+00	4.090e+03	6.857e+05	≈	4.799e+00	1.867e+01	2.940e+04	5.682e+00	9.168e+00	5.091e+00	5.404e+00
f_5	mean	1.910e+03	1.919e+03	1.903e+03	1.903e+03	1.906e+03	1.902e+03	≈	1.902e+03	1.903e+03	1.902e+03	1.902e+03	1.903e+03	1.902e+03	1.902e+03
	std	2.213e+00	2.903e+01	1.364e-12	9.095e-13	4.677e+00	4.933e+01	-	+	+	-	≈	≈	≈	+
f_6	mean	3.737e+03	2.086e+05	1.713e+03	4.092e+03	5.589e+03	2.835e+03	+	3.900e-01	4.614e-01	6.324e-01	4.918e-01	6.965e-01	4.325e-01	4.914e-01
	std	4.561e+02	2.235e+05	1.137e-12	4.547e-13	3.852e+03	1.043e+03	+	2.942e+03	4.545e+03	1.431e+03	1.396e+02	3.720e+03	6.811e+02	6.405e+01
f_7	mean	2.241e+03	1.017e+04	1.642e+03 ≈	2.171e+03	2.133e+08	1.828e+03	+	1.820e+03	2.115e+03	1.662e+03	1.773e+03	1.707e+03	1.831e+03	1.697e+03
	std	5.402e+02	8.067e+03	1.137e-12	1.364e-12	2.889e+08	1.711e+02	+	2.102e+02	2.201e+02	5.289e+01	1.340e+02	1.784e+02	2.343e+02	1.021e+02
f_8	mean	2.627e+04	1.961e+05	2.287e+03	8.117e+03	3.732e+03	3.668e+03	≈	1.167e+04	2.867e+04	1.056e+04	6.764e+03	1.775e+04	5.683e+03	3.540e+03
	std	1.074e+04	2.310e+05	4.547e-13	7.276e-12	1.176e+03	1.088e+03	+	+	+	+	+	+	+	≈
f_9	mean	2.314e+03	2.315e+03	2.305e+03	2.305e+03	2.972e+03	2.304e+03	+	4.881e+03	9.729e+03	2.332e+03	3.857e+03	1.162e+04	9.677e+03	1.185e+03
	std	6.943e-01	3.298e+00	1.819e-12	9.095e-13	2.082e+02	1.409e+00	≈	+	+	+	+	+	+	+
f_{10}	mean	3.450e+03	3.408e+03	2.616e+03	2.682e+03	3.035e+03	2.611e+03	+	2.594e+03	2.666e+03	2.600e+03	2.601e+03	2.595e+03	2.650e+03	2.583e+03
	std	3.080e+02	5.575e+02	9.095e-13	4.547e-13	5.205e+02	8.033e+00	+	+	+	+	+	+	+	+
f_{11}	mean	3.035e+03	3.085e+03	2.981e+03 ≈	2.982e+03	3.078e+03	2.996e+03	+	2.374e+01	9.837e+00	2.375e-01	5.057e+01	3.962e+01	2.800e+02	5.804e+01
	std	1.555e+01	6.064e+01	2.274e-12	4.547e-13	3.780e+01	1.395e+01	-	1.293e+01	3.983e+00	2.474e+00	1.250e+01	1.274e+01	1.381e+01	1.381e+01
$+/\approx/-:$	Avg. rank:	10/0/0	10/0/0	6/2/2	7/2/1	9/1/0	8/2/0	4/3/3	9/1/0	5/4/1	7/3/0	8/2/0	-	-	
	Avg. rank:	11.2	12.4	5.4	6.9	10.2	7.5	4.2	8.9	4.9	4.4	5.7	6.1	3.2	

Table 16 Results of comparison experiments in 20-D CEC2020

Func.	DE	PSO	CMA-ES	L-SHADE	jSO	L-SHADE-cnEpSIn	CSO	MCSO	L-SHACSO	CDE	CDEKI	ISHACDE	ASHADE-MPC
f_1 mean	5.262e+09	1.442e+09	2.563e+06	5.028e+03	9.980e+07	4.001e+07	+	1.208e+03	4.101e+05	4.015e+02	2.085e+02	5.680e+02	3.174e+02 1.043e+02
	+	+	+	+	+	+	+	+	+	+	+	+	+
f_2 std	7.082e+08	1.198e+09	9.313e-10	4.547e-12	1.360e+08	2.877e+07	+	1.361e+03	9.908e+04	3.738e+02	2.724e+02	7.112e+02	4.925e+02 1.255e+01
	+	+	+	+	+	+	-	+	+	+	+	3.859e+03	4.370e+03 3.009e+03
f_3 mean	5.368e+11	1.392e+11	5.397e+03	3.287e+03	5.035e+03	2.064e+09	+	1.482e+03	4.462e+03	1.251e+05	3.766e+02	6.855e+02	2.337e+02 3.236e+02
	+	+	+	+	+	+	-	+	+	+	+	-	-
f_4 std	1.116e+11	1.065e+11	4.547e-12	2.274e-12	1.431e+02	1.719e+09	+	2.481e+02	2.957e+02	1.325e+05	7.832e+02	7.782e+02	7.840e+02 7.739e+02
	+	+	+	+	+	+	-	+	+	+	+	~	+
f_5 mean	5.641e+10	2.007e+10	5.457e-12	1.137e-13	4.196e+03	2.732e+08	+	4.120e+00	1.022e+01	1.032e+04	2.732e+01	3.057e+01	1.783e+01 1.274e+01
	+	+	+	+	+	+	-	+	+	+	+	~	~
f_6 std	3.265e+03	6.614e+03	4.547e-13	1.592e-12	5.777e+00	1.487e+00	+	5.652e-01	9.582e-01	1.086e+00	2.228e+00	1.208e+00	9.027e-01
	+	+	+	+	+	+	-	+	+	+	+	+	+
f_7 mean	7.078e+05	6.744e+06	2.387e+03	1.811e+05	3.197e+04	3.492e+04	+	1.663e+05	2.393e+05	1.165e+05	1.737e+05	1.439e+05	4.528e+04 2.306e+04
	+	+	-	+	+	+	-	+	+	+	+	+	+
f_8 std	5.011e+05	4.616e+06	1.819e-12	1.455e-10	1.550e+04	1.455e+04	+	1.270e+05	8.759e+04	5.737e+04	1.243e+05	1.007e+05	8.766e+04 1.279e+04
	+	+	1.614e+03	2.627e+03	5.224e+05	3.900e+03	-	3.672e+03	3.305e+03	3.312e+03	1.652e+03	1.630e+03	1.887e+03 1.630e+03
f_9 mean	5.177e+03	1.329e+05	0.000e+00	9.095e-13	1.405e+06	1.545e+03	+	1.719e+03	9.693e+02	5.848e+02	1.038e+02	7.026e+01	1.353e+03 6.214e+01
	+	+	+	+	+	+	-	+	+	+	+	~	~
f_{10} std	9.685e+05	4.452e+06	2.280e+03	4.528e+04	3.154e+04	1.849e+04	+	1.019e+04	3.835e+04	1.003e+04	2.026e+04	1.523e+04	2.473e+04 6.039e+03
	+	+	-	+	+	+	-	+	+	+	+	+	~
f_9 mean	7.786e+03	6.577e+03	3.036e+03	2.601e+03	3.282e+03	2.894e+03	+	2.600e+03	2.644e+03	2.600e+03	2.600e+03	2.6222e+03	2.615e+03 2.608e+03
	+	+	+	+	+	+	-	+	+	+	+	+	+
f_{10} std	4.850e+02	2.869e+03	4.547e-13	2.274e-12	6.374e+02	1.350e+02	+	9.080e-04	4.917e+00	1.111e-01	4.129e-08	6.867e+01	5.942e+01 4.043e+01
	+	+	3.143e+03	3.146e+03	3.551e+03	3.347e+03	-	3.244e+03	3.159e+03	3.219e+03	3.269e+03	3.209e+03	3.208e+03 3.202e+03
f_{10} +/≈/- Avg. rank:	10/0/0	10/0/0	6/0/4	8/0/2	10/0/0	10/0/0	6/0/4	9/0/1	7/0/3	8/1/1	6/4/0	5/4/1	-
	12.2	12.3	6.2	6.1	9.9	8.9	4.5	7.1	5.3	5.7	5.4	4.7	2.7

D Detailed results of comparison experiments in CEC2022

Tables 17 and 18 summarize the detailed experimental results and statistical analysis in CEC2022 benchmark functions.

Table 17 Results of comparison experiments in 10-D CEC2022

Func.	DE	PSO	CMA-ES	L-SHADE	jSO	L-SHADE-cnEpSIn	CSO	MCSO	L-SHACSO	CDE	CDEKI	ISHACDIE	ASHADE-MPC	
f_1	mean	3.513e+03	1.204e+03	3.006e+02	3.326e+02	6.077e+02	3.040e+02	+	3.000e+02	3.399e+02	3.000e+02	3.000e+02	3.004e+02	
	std	9.125e+02	9.634e+02	1.137e-13	2.752e+02	1.576e+01	2.698e-04	+	+	1.630e+01	1.460e-03	8.611e-11	1.137e-14	
f_2	mean	4.249e+02	5.096e+02	4.089e+02	4.090e+02	4.314e+02	4.016e+02	-	4.080e+02	4.107e+02	4.009e+02	\approx	4.017e+02	
	std	8.575e+00	5.136e+01	5.684e-14	2.274e-13	3.701e+01	3.589e+00	+	+	1.372e+01	3.258e+00	4.356e+00	2.383e+00	9.964e+00
f_3	mean	6.000e+02	6.000e+02	6.000e+02	6.000e+02	6.000e+02	6.000e+02	+	6.000e+02	6.000e+02	6.000e+02	\approx	6.000e+02	
	std	4.599e-03	5.599e-03	4.547e-13	2.274e-13	2.211e-02	3.483e-05	+	+	1.453e-10	1.753e-05	2.297e-08	0.000e+00	0.000e+00
f_4	mean	8.010e+02	8.010e+02	8.767e+02	8.259e+02	8.003e+02	-	-	8.208e+02	8.409e+02	8.224e+02	\approx	\approx	
	std	2.269e-01	1.879e-01	5.684e-13	5.684e-13	2.676e+00	9.091e-02	-	9.000e+02	9.000e+02	9.000e+02	\approx	\approx	
f_5	mean	9.012e+02	9.012e+02	9.000e+02	9.001e+02	9.000e+02	9.000e+02	+	+	9.000e+02	9.000e+02	9.000e+02	\approx	9.000e+02
	std	3.512e-01	8.526e-01	7.958e-13	1.137e-12	3.662e-01	2.656e-02	+	+	2.041e-06	1.625e-03	7.504e-06	7.836e-02	2.491e-01
f_6	mean	3.443e+04	1.308e+06	1.825e+03	2.270e+04	1.412e+07	8.078e+03	+	+	1.195e+04	4.050e+04	1.095e+04	5.926e+03	1.319e+04
	std	1.022e+04	2.134e+06	1.592e-12	1.455e-11	4.664e+07	2.257e+03	+	+	4.225e+03	1.382e+04	3.032e+03	3.574e+03	8.137e+03
f_7	mean	2.042e+03	2.108e+03	2.057e+03	2.036e+03	2.041e+03	2.035e+03	+	2.027e+03	2.039e+03	2.030e+03	\approx	2.029e+03	
	std	1.006e+01	2.843e+01	1.364e-12	1.137e-12	2.962e+01	3.312e+00	+	-	1.963e+00	4.390e+00	2.567e+00	2.781e+00	4.390e+00
f_8	mean	2.234e+03	3.694e+03	2.223e+03	2.229e+03	9.314e+10	2.225e+03	+	+	2.259e+03	2.261e+03	2.237e+03	2.221e+03	2.2225e+03
	std	3.392e+00	1.670e+03	4.547e-13	1.364e-12	3.933e+11	8.306e-01	+	+	4.266e+01	2.706e+01	1.304e+01	6.693e+00	7.604e+00
f_9	mean	2.652e+03	2.603e+03	2.659e+03	2.304e+03	2.558e+03	2.301e+03	+	2.326e+03	2.304e+03	2.300e+03	\approx	\approx	
	std	6.775e+01	1.621e+02	1.364e-12	9.095e-13	2.074e+02	2.122e+00	+	+	9.175e+01	1.275e+00	8.264e-03	1.100e+02	1.321e+02
f_{10}	mean	2.617e+03	2.614e+03	2.622e+03	3.467e+03	2.601e+03	2.601e+03	+	+	2.653e+03	2.624e+03	2.624e+03	\approx	\approx
	std	9.846e+00	6.652e+00	2.274e-12	1.819e-12	5.553e+02	1.543e+00	+	+	4.541e+01	1.002e+00	1.307e+01	2.341e+01	5.153e+01
f_{11}	mean	2.662e+03	2.624e+03	3.476e+03	2.601e+03	2.613e+03	2.600e+03	+	+	2.600e+03	2.601e+03	2.600e+03	2.600e+03	2.600e+03
	std	1.869e+02	1.733e+01	1.819e-12	2.274e-12	1.180e+01	1.845e-01	+	+	1.869e-03	1.837e-01	3.271e-03	1.480e-08	7.440e-04
f_{12}	mean	2.867e+03	2.906e+03	2.864e+03	2.867e+03	4.253e+03	2.869e+03	+	+	2.867e+03	2.867e+03	2.867e+03	\approx	\approx
	std	1.571e+00	1.690e+01	2.274e-12	0.000e+00	3.031e+02	1.642e+00	+	+	8.524e-01	2.356e-01	6.550e-01	3.074e+00	9.016e+00
	+/-/≈/-:	9/1/2	10/0/2	9/0/3	11/0/1	12/0/0	9/0/3	10/0/2	10/1/1	9/1/2	5/5/2	7/4/1	9/3/0	-
Avg. rank:	9.3	10.3	7.4	7.8	11.8	5.7	5.8	8.5	4.7	6.8	5.2	3.2		

Table 18 Results of comparison experiments in 20-D CFC2022

Func.	DE	PSO	CMA-ES	L-SHADE	jSO	L-SHADE-cnEpsin	CSO	MCSO	L-SHACSO	CDE	CDEKI	ISHACDE	ASHADE-MPC	
f_1	mean	2.327e+04	1.482e+04	3.576e+02	3.131e+02	6.543e+02	5.769e+02	+	3.000e+02	3.449e+02	3.000e+02	3.000e+02	5.557e+02	
	std	+ 3.345e+03	8.401e+03	1.137e-13	1.705e-13	4.164e+02	1.644e+02	+ 6.763e-05	1.306e+01	9.384e-04	~ 1.224e-11	2.542e-14	1.505e+03	
f_2	mean	7.487e+02	7.443e+02	4.299e+02	4.492e+02	5.304e+02	4.793e+02	+ -	-	4.535e+02	4.526e+02	4.540e+02	4.519e+02	
	std	+ 6.734e+01	2.509e+02	2.842e-13	3.411e-13	4.321e+01	1.230e+01	- -	-	-	-	-	4.540e+02	
f_3	mean	6.002e+02	6.001e+02	6.000e+02	6.000e+02	6.000e+02	6.000e+02	+ +	6.000e+02	6.000e+02	6.000e+02	6.000e+02	6.000e+02	
	std	+ 3.664e+02	6.139e+02	2.274e-13	2.274e-13	1.158e-02	3.299e-03	+ 9.534e+02	6.016e-14	2.368e-06	+ 8.306e+02	3.398e-09	5.332e-14	
f_4	mean	8.041e+02	8.039e+02	9.983e+02	9.711e+02	8.017e+02	-	+ -	9.633e+02	8.383e+02	+ 9.820e+02	9.939e+02	9.803e+02	
	std	+ 3.468e-01	4.087e-01	1.251e-12	2.274e-13	9.227e+00	3.459e-01	- -	7.258e+00	2.127e+01	-	+ 9.004e+02	2.104e+01	
f_5	mean	9.110e+02	9.078e+02	9.004e+02	9.005e+02	9.021e+02	9.001e+02	+ +	9.000e+02	9.000e+02	+ 9.004e+02	9.004e+02	9.001e+02	
	std	+ 2.612e+00	3.920e+00	4.547e-13	9.095e-13	3.238e-01	6.763e-02	- -	-	-	-	-	3.151e+01	
f_6	mean	1.085e+08	3.323e+08	7.089e+03	1.153e+06	2.240e+04	2.613e+04	- -	3.438e+04	1.593e+06	-	+ +	9.000e+02	
	std	+ 6.421e+07	2.846e+08	7.276e-12	6.985e-10	5.144e+03	3.785e+03	- -	6.458e-02	2.749e-04	-	+ +	1.005e-01	
f_7	mean	2.616e+03	3.003e+03	2.085e+03	2.074e+03	2.179e+03	2.048e+03	\approx	- -	8.320e+03	6.281e+05	-	+ +	2.453e+01
	std	+ 2.342e+02	5.676e+02	4.547e-13	9.095e-13	2.095e+02	9.429e+00	- -	- -	2.027e+03	2.047e+03	\approx	+ +	2.332e+05
f_8	mean	1.102e+04	6.292e+07	2.232e+03	3.104e+03	2.409e+03	2.428e+03	+ -	3.158e+03	4.045e+03	3.105e+03	-	3.047e+03	
	std	+ 6.998e+03	1.475e+08	2.728e-12	4.547e-13	1.985e+02	1.558e+02	- -	4.459e+02	6.068e+02	2.751e+02	-	2.048e+03	
f_9	mean	2.691e+03	3.264e+03	2.639e+03	2.650e+03	2.592e+03	2.674e+03	+ -	2.643e+03	2.648e+03	2.647e+03	-	2.627e+03	
	std	+ 2.304e+01	2.632e+02	0.000e+00	1.819e-12	1.567e+02	8.016e+01	- -	4.941e+01	3.046e+00	2.932e+00	-	1.257e+01	
f_{10}	mean	4.159e+03	2.833e+03	3.011e+03	2.841e+03	5.712e+03	2.769e+03	- -	2.833e+03	2.824e+03	2.802e+03	-	2.366e+01	
	std	+ 1.833e+03	3.222e+01	0.000e+00	3.6338e-12	1.935e+02	3.176e+00	- -	3.105e+03	3.105e+03	3.105e+03	-	1.899e+01	
f_{11}	mean	3.204e+03	2.723e+03	2.621e+03	2.600e+03	2.603e+03	2.769e+03	- -	2.802e+03	2.802e+03	2.802e+03	-	7.739e+00	
	std	+ 5.957e+02	1.014e+02	1.819e-12	1.364e-12	5.656e+00	2.524e+00	- -	4.941e+01	1.341e+01	1.341e+01	-	1.206e+03	
f_{12}	mean	2.953e+03	3.257e+03	2.945e+03	\approx	2.949e+03	2.983e+03	+ +	2.954e+03	2.946e+03	2.949e+03	-	5.558e+01	
	std	+ 1.300e+01	8.922e+01	4.547e-13	2.728e-12	7.559e+01	1.686e+01	- -	1.026e+01	5.613e+00	7.614e+00	-	1.206e+03	
+/ \approx -:		11/0/1	11/0/1	8/1/3	10/1/1	10/0/2	8/1/3	-	7/1/4	7/3/2	6/1/5	-	7/5/0	
Avg. rank:	11.2	11.1	6.5	7.3	8.8	6.6	5.5	6.6	4.4	6.4	6.9	5.9	3.7	

Acknowledgements This work is supported by the project of the School of Tropical Crops, Yunnan Agricultural University (No. 2023RYYB003) and Scientific Research Fund Project of Education Department of Yunnan Province (No. 2025J0385).

Author Contributions Zhongmin Wang: Conceptualization, Methodology, Software, Writing – original draft, and Writing – review & editing. Qifang Luo: Investigation, Methodology, Formal Analysis, and Writing – review & editing. Chuan Zhang: Investigation, Methodology, Formal Analysis, and Writing – review & editing. Xuejun Li: Investigation, Methodology, Formal Analysis, and Writing – review & editing. Shiwei Chen: Investigation, Methodology, Formal Analysis, and Writing – review & editing. Hantang Li: Investigation, Methodology, Formal Analysis, and Writing – review & editing. Jun Yu: Resources and Writing – review & editing. Mahmoud Abdel-Salam: Resources, Formal Analysis, and Writing – review & editing. Rui Zhong: Supervisor, Project administration, and Writing – review & editing. Daihong Li: Investigation, Methodology, Formal Analysis, and Writing – review & editing.

Data Availability The source code of this research can be downloaded at <https://github.com/RuiZhong961230/ASHADE-MPC>.

Declarations

Competing interest The authors declare no competing interests.

References

- Abdel-Basset, M., Abdel-Fatah, L., Sangaiah, A.K.: Metaheuristic algorithms: a comprehensive review. *Comput. Int. Mult. Big Data Cloud Eng. Appl.* 185–231 (2018)
- Dokeroglu, T., Sevinc, E., Kucukyilmaz, T., Cosar, A.: A survey on new generation metaheuristic algorithms. *Computers & Industrial Engineering* **137**, 106040 (2019)
- Prity, F.S.: Nature-inspired optimization algorithms for enhanced load balancing in cloud computing: a comprehensive review with taxonomy, comparative analysis, and future trends. *Swarm and Evolutionary Computation* **97**, 102053 (2025)
- Jia, H., Lu, C.: Guided learning strategy: a novel update mechanism for metaheuristic algorithms design and improvement. *Knowledge-Based Systems* **286**, 111402 (2024)
- Barua, S., Merabet, A.: Lévy arithmetic algorithm: an enhanced metaheuristic algorithm and its application to engineering optimization. *Expert Systems with Applications* **241**, 122335 (2024)
- López, B., Moreno, L., Monje, C.A.: Dgs-edo: a double-guided sampling estimation of distribution algorithm for multi-robot task assignment as a permutation optimization problem. *Swarm and Evolutionary Computation* **98**, 102112 (2025)
- Ramanjaiah, G., Kiran, T.S.R., Srisaila, A., Lakshmanarao, A., Ramakrishna, K.V.S.S., Rao, K.V.: Secure key based cloud security utilizing three-way protection with martino homomorphic encryption for preventing unauthorized data access. *Swarm and Evolutionary Computation* **98**, 102131 (2025)
- Khayamim, R., Moses, R., Ozguven, E.E., Borowska-Stefanska, M., Wiśniewski, S., Dulebenets, M.A.: Swarm intelligence applications for emergency evacuation planning: state of the art, recent developments, and future research opportunities. *Swarm and Evolutionary Computation* **96**, 102009 (2025)
- Tomar, V., Bansal, M., Singh, P.: Metaheuristic algorithms for optimization: a brief review. *Eng. Proc.* **59**(1), 238 (2024)
- Eltaeib, T., Mahmood, A.: Differential evolution: a survey and analysis. *Applied Sciences* **8**(10), 1945 (2018)
- Song, Y., Zhao, G., Zhang, B., Chen, H., Deng, W., Deng, W.: An enhanced distributed differential evolution algorithm for portfolio optimization problems. *Engineering Applications of Artificial Intelligence* **121**, 106004 (2023)
- Gu, Q., Li, S., Liao, Z.: Solving nonlinear equation systems based on evolutionary multitasking with neighborhood-based speciation differential evolution. *Expert Systems with Applications* **238**, 122025 (2024)
- Jin, X.L., Zhang, S.X., Zheng, L.M., Zheng, S.Y.: Differential evolution algorithm with local and global parameter adaptation. *Swarm and Evolutionary Computation* **98**, 102125 (2025)
- Adam, S.P., Alexandropoulos, S.-A.N., Pardalos, P.M., Vrahatis, M.N.: No free lunch theorem: a review. *Approx. Optim.: Algorithm. Complex.* 57–82 (2019)
- Ahmad, M.F., Isa, N.A.M., Lim, W.H., Ang, K.M.: Differential evolution: a recent review based on state-of-the-art works. *Alexandria Engineering Journal* **61**(5), 3831–3872 (2022)
- Ye, X., Li, J., Wang, P., Suganthan, P.N.: A comprehensive survey of adaptive strategies in differential evolutionary algorithms. *Swarm and Evolutionary Computation* **98**, 102081 (2025)
- Zhang, J., Sanderson, A.C.: Jade: adaptive differential evolution with optional external archive. *IEEE Trans. Evol. Comput.* **13**(5), 945–958 (2009)
- Wang, X., Li, C., Zhu, J., Meng, Q.: L-shade-e: ensemble of two differential evolution algorithms originating from l-shade. *Information Sciences* **552**, 201–219 (2021)
- Ghosh, A., Das, S., Das, A.K., Senkerik, R., Viktorin, A., Zelinka, I., Masegosa, A.D.: Using spatial neighborhoods for parameter adaptation: an improved success history based differential evolution. *Swarm and Evolutionary Computation* **71**, 101057 (2022)
- Yang, J., Wang, K., Wang, Y., Wang, J., Lei, Z., Gao, S.: Dynamic population structures-based differential evolution algorithm. *IEEE Trans. Emerg. Top. Comput. Intell.* **8**(3), 2493–2505 (2024)
- Tanabe, R., Fukunaga, A.: Success-history based parameter adaptation for differential evolution, In: 2013 IEEE congress on evolutionary computation, IEEE, pp. 71–78 (2013)
- Aggarwal, S., Mishra, K.K.: X-mode: extended multi-operator differential evolution algorithm. *Mathematics and Computers in Simulation* **211**, 85–108 (2023)
- Mohamed, A.W., Hadi, A.A., Jambi, K.M.: Novel mutation strategy for enhancing shade and lshade algorithms for global numerical optimization. *Swarm and Evolutionary Computation* **50**, 100455 (2019)
- Yang, Q., Qiao, Z.-Y., Xu, P., Lin, X., Gao, X.-D., Wang, Z.-J., Lu, Z.-Y., Jeon, S.-W., Zhang, J.: Triple competitive differential evolution for global numerical optimization. *Swarm and Evolutionary Computation* **84**, 101450 (2024)
- Zhong, R., Cao, Y., Zhang, E., Munetomo, M.: Introducing competitive mechanism to differential evolution for numerical optimization, arXiv preprint [arXiv:2406.05436](https://arxiv.org/abs/2406.05436) (2024)
- Abd Elaziz, M., Yang, H., Lu, S.: A multi-leader harris hawk optimization based on differential evolution for feature selection and prediction influenza viruses h1n1. *Artif. Intell. Rev.* **55**(4), 2675–2732 (2022)
- Gao, Q., Sun, H., Wang, Z.: Dp-epso: differential privacy protection algorithm based on differential evolution and particle swarm optimization. *Optics & Laser Technology* **173**, 110541 (2024)
- Hansen, N., Ostermeier, A.: Completely derandomized self-adaptation in evolution strategies. *Evol. Comput.* **9**(2), 159–195 (2001)
- Tanabe, R., Fukunaga, A.S.: Improving the search performance of shade using linear population size reduction, In: 2014 IEEE Congress on Evolutionary Computation (CEC), pp. 1658–1665 (2014)
- Brest, J., Maučec, M.S., Bošković, B.: Single objective real-parameter optimization: algorithm JSO, In: 2017 IEEE congress

- on evolutionary computation (CEC), IEEE, pp. 1311–1318 (2017)
- 31. Awad, N.H., Ali, M.Z., Suganthan, P.N.: Ensemble sinusoidal differential covariance matrix adaptation with euclidean neighborhood for solving cec2017 benchmark problems, In: 2017 IEEE congress on evolutionary computation (CEC), IEEE, pp. 372–379 (2017)
 - 32. Storn, R., Price, K.: Differential evolution - a simple and efficient heuristic for global optimization over continuous spaces. *Journal of Global Optimization* **11**, 341–359 (1997)
 - 33. Brest, J., Maučec, M.S., Bošković, B.: Single objective real-parameter optimization: algorithm JSO, In: 2017 IEEE Congress on Evolutionary Computation (CEC), pp. 1311–1318 (2017)
 - 34. Awad, N.H., Ali, M.Z., Suganthan, P.N., Reynolds, R.G.: An ensemble sinusoidal parameter adaptation incorporated with l-shade for solving cec2014 benchmark problems, In: 2016 IEEE congress on evolutionary computation (CEC), IEEE, pp. 2958–2965 (2016)
 - 35. Mohamed, A.W., Hadi, A.A., Jambi, K.M.: Novel mutation strategy for enhancing shade and lshade algorithms for global numerical optimization. *Swarm and Evolutionary Computation* **50**, 100455 (2019)
 - 36. Stanovov, V., Akhmedova, S., Semenkin, E.: Nl-shade-rsp algorithm with adaptive archive and selective pressure for CEC 2021 numerical optimization, In: 2021 IEEE Congress on Evolutionary Computation (CEC), IEEE, pp. 809–816 (2021)
 - 37. Kumar, A., Biswas, P.P., Suganthan, P.N.: Differential evolution with orthogonal array-based initialization and a novel selection strategy. *Swarm and Evolutionary Computation* **68**, 101010 (2022)
 - 38. Zhong, R., Hussien, A.G., Zhang, S., Xu, Y., Yu, J.: Space mission trajectory optimization via competitive differential evolution with independent success history adaptation. *Applied Soft Computing* **171**, 112777 (2025)
 - 39. Wang, D., Tan, D., Liu, L.: Particle swarm optimization algorithm: an overview. *Soft. Comput.* **22**(2), 387–408 (2018)
 - 40. Cheng, R., Jin, Y.: A competitive swarm optimizer for large scale optimization. *IEEE Trans. Cybern.* **45**(2), 191–204 (2015)
 - 41. Mohapatra, P., Das, K.N., Roy, S.: A modified competitive swarm optimizer for large scale optimization problems. *Applied Soft Computing* **59**, 340–362 (2017)
 - 42. Zhong, R., Wang, Z., Hussien, A.G., Houssein, E.H., Al-Shourbaji, I., Elseify, M.A., Yu, J.: Success history adaptive competitive swarm optimizer with linear population reduction: performance benchmarking and application in eye disease detection. *Comput. Biol. Med.* **186**, 109587 (2025)
 - 43. Stanovov, V., Akhmedova, S., Semenkin, E.: Lshade algorithm with rank-based selective pressure strategy for solving CEC 2017 benchmark problems, In: 2018 IEEE Congress on Evolutionary Computation (CEC), pp. 1–8 (2018)
 - 44. Mohamed, A.W., Hadi, A.A., Mohamed, A.K., Awad, N.H.: Evaluating the performance of adaptive gainingsharing knowledge based algorithm on CEC 2020 benchmark problems, In: 2020 IEEE Congress on Evolutionary Computation (CEC), pp. 1–8 (2020)
 - 45. Bujok, P., Kolenovsky, P.: Eigen crossover in cooperative model of evolutionary algorithms applied to CEC 2022 single objective numerical optimisation, In: 2022 IEEE Congress on Evolutionary Computation (CEC), pp. 1–8 (2022)
 - 46. Midway, S., Robertson, M., Flinn, S., Kaller, M.: Comparing multiple comparisons: practical guidance for choosing the best multiple comparisons test. *PeerJ* **8**, e10387 (2020)
 - 47. Zimmerman, D.W., Zumbo, B.D.: Relative power of the wilcoxon test, the friedman test, and repeated-measures anova on ranks. *The Journal of Experimental Education* **62**(1), 75–86 (1993)
 - 48. Li, K., Huang, H., Fu, S., Ma, C., Fan, Q., Zhu, Y.: A multi-strategy enhanced northern goshawk optimization algorithm for global optimization and engineering design problems. *Computer Methods in Applied Mechanics and Engineering* **415**, 116199 (2023)
 - 49. López-Arcadia, C.A., Bonilla-Moheno, M., Porter-Bolland, L., Hernández-Martínez, G.: Transformation of the coffee-growing landscape in central veracruz, mexico: collaboration, markets, and farmer characteristics mediate the effects of the coffee-leaf rust outbreak. *Reg. Environ. Change* **25**(1), 1–16 (2025)
 - 50. Koutouleas, A., Collinge, D.B., Boa, E.: The coffee leaf rust pandemic: an ever-present danger to coffee production. *Plant Pathology* **73**(3), 522–534 (2024)
 - 51. Krizhevsky, A., Sutskever, I., Hinton, G.E.: Imagenet classification with deep convolutional neural networks, In: Pereira, F., Burges, C., Bottou, L., Weinberger, K. (eds.), *Advances in Neural Information Processing Systems*, Vol. 25, Curran Associates, Inc., (2012)
 - 52. He, K., Zhang, X., Ren, S., Sun, J.: Deep residual learning for image recognition (2015). [arXiv:1512.03385](https://arxiv.org/abs/1512.03385)
 - 53. Simonyan, K., Zisserman, A.: Very deep convolutional networks for large-scale image recognition (2015). [arXiv:1409.1556](https://arxiv.org/abs/1409.1556)
 - 54. Szegedy, C., Ioffe, S., Vanhoucke, V., Alemi, A.: Inception-v4, inception-resnet and the impact of residual connections on learning, In: Proceedings of the AAAI conference on artificial intelligence, Vol. 31, (2017)
 - 55. Sandler, M., Howard, A., Zhu, M., Zhmoginov, A., Chen, L.-C.: Mobilenetv2: Inverted residuals and linear bottlenecks (2019). [arXiv:1801.04381](https://arxiv.org/abs/1801.04381)
 - 56. Liu, Z., Lin, Y., Cao, Y., Hu, H., Wei, Y., Zhang, Z., Lin, S., Guo, B.: Swin transformer: hierarchical vision transformer using shifted windows, In: Proceedings of the IEEE/CVF International Conference on Computer Vision (ICCV), pp. 10012–10022 (2021)
 - 57. Liu, Z., Mao, H., Wu, C.-Y., Feichtenhofer, C., Darrell, T., Xie, S.: A convnet for the 2020s, Proceedings of the IEEE/CVF Conference on Computer Vision and Pattern Recognition (CVPR) (2022)
 - 58. Paszke, A., Gross, S., Massa, F., Lerer, A., Bradbury, J., Chanan, G., Killeen, T., Lin, Z., Gimelshein, N., Antiga, L., Desmaison, A., Kopf, A., Yang, E., DeVito, Z., Raison, M., Tejani, A., Chilamkurthy, S., Steiner, B., Fang, L., Bai, J., Chintala, S.: Pytorch: An imperative style, high-performance deep learning library, In: Wallach, H., Larochelle, H., Beygelzimer, A., d'Alché-Buc, F., Fox, E., Garnett, R. (eds.), *Advances in Neural Information Processing Systems*, Vol. 32, Curran Associates, Inc., (2019)

Publisher's Note Springer Nature remains neutral with regard to jurisdictional claims in published maps and institutional affiliations.

Springer Nature or its licensor (e.g. a society or other partner) holds exclusive rights to this article under a publishing agreement with the author(s) or other rightsholder(s); author self-archiving of the accepted manuscript version of this article is solely governed by the terms of such publishing agreement and applicable law.